

# Determining Modes for Continuous Data Assimilation in 2D Turbulence

ERIC OLSON<sup>1,2</sup> and EDRISS S. TITI<sup>1,3,4</sup>

We study the number of determining modes necessary for continuous data assimilation in the two-dimensional incompressible Navier–Stokes equations. Our focus is on how the spatial structure of the body forcing affects the rate of continuous data assimilation and the number of determining modes. These quantities are shown to depend strongly on the length scales present in the forcing.

*Dedicated to the memory of Oscar P. Manley*

## 1. Introduction

In the late 1960s satellite-borne observation systems began producing data on the climate that was nearly continuous in time. Charney, Halem and Jastrow proposed in [5] that the equations of the atmosphere themselves be used to process this data and obtain improved estimates of the current atmospheric state. Their method, called *continuous data assimilation*, is to insert the observational measurements directly into a model as the latter is being integrated in time. A summary of the use of continuous data assimilation in practical weather forecasting appears in Daley [12].

Let  $u_1(t)$  represent physical reality at time  $t$ . We represent the observational measurements corresponding to  $u_1(t)$  at time  $t$  by  $P_\lambda u_1(t)$ , where  $P_\lambda$  is a finite-rank orthogonal projection. Here  $\lambda$  represents a parameter, namely the resolution of the measuring equipment, that will be made precise later. Let  $u_2(t)$  be the approximation to  $u_1(t)$  obtained from continuous data assimilation of the observational measurements  $P_\lambda u_1(\tau)$  over the time interval  $\tau \in [0, t]$ . We will describe the details of constructing  $u_2(t)$  later. Our goal is to find conditions on  $\lambda$  in terms of the other physical parameters of the system which guarantee that  $u_2(t)$  will converge to  $u_1(t)$  as  $t \rightarrow \infty$ . Note that we assume the idealized situation in which the observational measurements  $P_\lambda u_1(t)$  are error free; therefore, there is no need for the additional filtering necessary in applications.

Inspired by the work of Browning, Henshaw and Kreiss [2] and motivated by applications involving the full dynamics of the atmosphere, we study continuous data

---

<sup>1</sup> Department of Mathematics, University of California, Irvine CA 92697, USA

<sup>2</sup> Department of Mathematics, University of Nevada, Reno NV 89557, USA

<sup>3</sup> Mechanical and Aerospace Engineering, University of California, Irvine CA 92697, USA

<sup>4</sup> Department of Computer Science and Applied Mathematics, Weizmann Institute of Science, Rehovot 76100, Israel

assimilation in the simpler case of a viscous two-dimensional incompressible fluid in a periodic domain. Thus, we take the physical reality  $u_1(t)$  to be the exact solution of the two-dimensional incompressible Navier–Stokes equations

$$\frac{\partial u_1}{\partial t} + (u_1 \cdot \nabla)u_1 - \nu \Delta u_1 + \nabla \pi_1 = f, \quad \nabla \cdot u_1 = 0 \quad (1.1)$$

with initial conditions  $u_1(0) = u_0$  on the  $L$ -periodic torus  $\Omega = [0, L]^2$ . Here  $u_1$  represents the Eulerian velocity field,  $\nu$  the kinematic viscosity,  $f$  a body forcing and  $\pi_1$  the physical pressure.

It is clear from (1.1) that if  $\int_{\Omega} u_0 = 0$  and  $\int_{\Omega} f = 0$ , then  $\int_{\Omega} u_1(t) = 0$  for all time. Therefore, we consider only solutions with zero mean. It follows that at any time  $t$  the velocity field, the body forcing and the pressure may each be represented by a Fourier series of the form

$$a = \sum_{k \in \mathcal{J}} \hat{a}_k \phi_k, \quad \text{where} \quad \mathcal{J} = \left\{ \frac{2\pi m}{L} : m \in \mathbf{Z}^2 \setminus \{0\} \right\}, \quad (1.2)$$

$\phi_k(x) = e^{ik \cdot x}$  and  $\hat{a}_k = \overline{\hat{a}_{-k}}$ . Note that the Fourier coefficients corresponding to the velocity and the forcing are  $\mathbf{C}^2$ -vector valued such that  $k \cdot \hat{a}_k = 0$  whereas the coefficients corresponding to the pressure are scalar. Define the norms

$$|a| = L \left\{ \sum_{k \in \mathcal{J}} |\hat{a}_k|^2 \right\}^{1/2} \quad \text{and} \quad \|a\| = L \left\{ \sum_{k \in \mathcal{J}} |k|^2 |\hat{a}_k|^2 \right\}^{1/2}. \quad (1.3)$$

The Fourier space representation provides a convenient way of describing the orthogonal projections needed for our study. For  $a$  such that  $|a| < \infty$  we define

$$P_{\lambda} a = \sum_{|k|^2 \leq \lambda} \hat{a}_k \phi_k \quad \text{and} \quad Q_{\lambda} = I - P_{\lambda}. \quad (1.4)$$

Thus, for the projection  $P_{\lambda} u_1(t)$  given above, the quantity  $\lambda^{-1/2}$  represents the smallest length scale of the fluid which can be observed—the resolution of the presumed measuring equipment. Note that  $\lambda$  and the rank  $N$  of  $P_{\lambda}$  are essentially proportional in two dimensions.

In light of the results on determining projections postulated by Foias and Temam in [25] and proven in [6, 7, 28], similar results to those we shall present here are likely to hold for any family of projections  $P_{\lambda}$  for which there exists constants  $C_1$  and  $\gamma > 0$  not depending on the rank  $N$  of  $P_{\lambda}$  such that  $\|u - P_{\lambda} u\| \leq C_1 N^{-\gamma} \|u\|$  for all  $u$  such that  $\|u\| < \infty$ . See also [8] and [32]. Further work along these lines appears in [4] for the physically relevant model consisting of the two-dimensional Navier–Stokes equations on the surface of a rotating sphere.

Let us agree that if we were given  $u_0$  exactly, that is, the detailed reality at time  $t = 0$ , then we could integrate the Navier–Stokes equations and hence get  $u_1(t)$  exactly for any  $t > 0$ . Therefore, the main difficulty is that we can not obtain  $u_0$  exactly by

measurement. However, we can obtain  $P_\lambda u_1(t)$  over as large an interval in time as needed. The question becomes, how do we find  $u_1(t)$  from  $P_\lambda u_1(t)$ . In general this is not possible, so alternatively, let us find  $u_2(t)$ , a good asymptotic approximation of  $u_1(t)$ .

To motivate finding  $u_2(t)$  let us rewrite the Navier–Stokes equations (1.1) as a system of two coupled differential equations. Let  $u_i = p_i + q_i$  where  $p_i = P_\lambda u_i$  and  $q_i = Q_\lambda u_i$  for  $i = 1, 2$ . Since  $P_\lambda$  and  $Q_\lambda$  project onto eigenfunctions of the  $\Delta$  operator then they commute with it. Similarly  $P_\lambda$  and  $Q_\lambda$  commute with the divergence and the gradient. Thus, projecting (1.1) by  $P_\lambda$  and then by  $Q_\lambda$  gives

$$\begin{cases} \frac{\partial p_1}{\partial t} + P_\lambda \{(p_1 + q_1) \cdot \nabla(p_1 + q_1)\} - \nu \Delta p_1 + \nabla P_\lambda \pi_1 = P_\lambda f, & \nabla \cdot p_1 = 0 \\ \frac{\partial q_1}{\partial t} + Q_\lambda \{(p_1 + q_1) \cdot \nabla(p_1 + q_1)\} - \nu \Delta q_1 + \nabla Q_\lambda \pi_1 = Q_\lambda f, & \nabla \cdot q_1 = 0. \end{cases}$$

Since  $p_1(t)$  is given directly by measurement, we need only integrate the second equation to find  $u_1(t)$ . However, since we do not know  $q_1(0)$  then integrating the second equation is impossible. Therefore, we compute an approximation  $q_2(t)$  of  $q_1(t)$  by integrating

$$\frac{\partial q_2}{\partial t} + Q_\lambda \{(p_1 + q_2) \cdot \nabla(p_1 + q_2)\} - \nu \Delta q_2 + \nabla Q_\lambda \pi_2 = Q_\lambda f, \quad \nabla \cdot q_2 = 0 \quad (1.5)$$

with initial conditions  $q_2(0) = \eta$  where  $\eta = Q_\lambda \eta$  represents an initial guess of the high modes  $q_1(0)$  of the exact solution. Hence, the problem for us is a problem of initialization, and we solve it by initializing the high frequencies any way we want and then integrating.

In the numerical part of this paper we simply take  $\eta = 0$ , however, an initial approximation of  $q_1(0)$  might be more reasonably obtained by taking  $\eta = Q_\lambda \Phi(p_1(0))$  where  $\Phi$  is an approximate inertial manifold for the two-dimensional Navier–Stokes equations. More information on approximate inertial manifolds and their applications may be found in Debussche and Marion [13], Devulder and Marion [14], Dubios, Jauberteau and Temam [17], Foias, Manley and Temam [19, 20] and [15], [18], [23], [30], [42] and references therein.

A systematic computational study of continuous data assimilation in decaying two-dimensional turbulence was first performed by Browning, Henshaw and Kreiss [2]. In [2], computations were done on the  $2\pi$ -periodic torus with viscosity  $\nu = 10^{-5}$ , forcing  $f = 0$  and  $\eta = 0$ . First, a highly accurate reference calculation was made to obtain the solution  $u_1(t)$  of (1.1) starting from prescribed initial conditions  $u_0$  such that  $|u_0| = 1$ . The observational measurements  $P_\lambda u_1(t)$  were saved and subsequently used for assimilation into a second calculation to obtain  $u_2(t)$ . Notice that since the forcing is zero, both  $u_1$  and  $u_2$  eventually converge to zero. However, short time transient behavior may be studied, for example, by monitoring the relative error  $|u_1(t) - u_2(t)|/|u_1(t)|$ . Under these conditions, it was observed in [2] that continuous data assimilation of the 64 lowest Fourier modes of  $u_1$  was sufficient to accurately reconstruct the small scales of  $u_1$ , but assimilation of the 16 lowest modes was not.

A similar study of decaying three-dimensional turbulence was recently completed by Kreiss and Yström in [33]. In this paper we generalize [2] by considering a non-zero body forcing  $f$  to avoid the difficulties of  $u_1$  and  $u_2$  decaying to zero.

Continuous data assimilation is essentially the simplest algorithm for constructing an approximate solution  $u_2$  suitable for treatment by the theory of determining modes of Foias and Prodi [22]. In this context it is necessary to view  $u_2$  as a solution to a modified two-dimensional Navier–Stokes equations. This may be done by adding the evolution equations for  $p_1(t)$  to the evolution equations for  $q_2(t)$ . Thus, we obtain

$$\frac{\partial u_2}{\partial t} + (u_2 \cdot \nabla)u_2 - \nu \Delta u_2 + \nabla \pi_2 = f_2, \quad \nabla \cdot u_2 = 0 \quad (1.6)$$

with initial conditions  $u_2(0) = P_\lambda u_0 + \eta$  where  $\eta = Q_\lambda \eta$  and

$$f_2 = f + P_\lambda \{(u_2 \cdot \nabla)u_2 - (u_1 \cdot \nabla)u_1\}. \quad (1.7)$$

Note that  $f_2$  is a complicated time-dependent feedback forcing function that depends on  $u_2$  to ensure that  $P_\lambda u_1(t) = P_\lambda u_2(t)$  for all time  $t \geq 0$ .

The theory of determining modes, however, makes no assumptions on how  $u_2$  was obtained. So, for a moment, let us forget that  $u_2$  was constructed by continuous data assimilation and simply suppose it to be another solution to the Navier–Stokes equations with a given time dependent forcing  $f_2(t)$ . To avoid possible confusion we shall refer to independent solutions of the standard incompressible two-dimensional Navier–Stokes equations (1.1) by  $v_1$  and  $v_2$  and their corresponding forcing functions by  $g_1$  and  $g_2$  when discussing the general theory of determining modes.

**Definition 1.1.** The *number of determining modes* is the rank of the smallest projection  $P_\lambda$  such that for any two solutions  $v_1$  and  $v_2$  of (1.1) the convergence  $|P_\lambda v_1(t) - P_\lambda v_2(t)| \rightarrow 0$  as  $t \rightarrow \infty$  guarantees that  $|v_1(t) - v_2(t)| \rightarrow 0$  as  $t \rightarrow \infty$ . We denote by  $\lambda_c$  the smallest value of  $\lambda$  such that the rank of  $P_\lambda$  is equal to the number of determining modes  $N_c$ .

It was first shown in [22] that the two-dimensional Navier–Stokes equations possess a finite number of determining modes. At about the same time a result more directly related to continuous data assimilation was independently proved by Ladyzhenskaya [35]. It is clear that the number of determining modes should depend on the forcing, the viscosity, and the size of the domain. In [43] Trève and Manley gave a physical argument relating the number of determining modes in Rayleigh–Bénard convection to the Rayleigh number divided by the Prandtl number. By identifying the buoyancy force in Rayleigh–Bénard convection with the body forcing in the Navier–Stokes equations this lead to

**Definition 1.2.** The *Grashof number* is defined as

$$\text{Gr}(f) = (L/2\pi\nu)^2 \limsup_{t \rightarrow \infty} |f(t)|.$$

The first reasonable rigorous estimate on the number of determining modes in terms of the Grashof number was provided by Foias, Manley, Temam and Trève [21]. It

was observed by Foias and Temam in [24] and in [31] that the theory of determining modes can be extended to families of Navier–Stokes equations with asymptotically equivalent body forcing. This is of particular interest to us, since the forcing function  $f_2$  in continuous data assimilation is not equal to  $f$ . The best estimate to date in the periodic case is given in [32] which we shall restate here as

**Theorem 1.3.** *Let  $v_1$  and  $v_2$  be two solutions of the two-dimensional Navier–Stokes equations on the  $L$ -periodic torus with corresponding forcing functions  $g_1$  and  $g_2$  and possibly different initial conditions. Then there exists a constant  $c_1$  independent of  $\nu$ ,  $L$ ,  $g_i$  or of any initial conditions such that for every  $\lambda(L/2\pi)^2 > c_1\text{Gr}(g_1)$  the limits*

$$|g_1(t) - g_2(t)| \rightarrow 0 \quad \text{and} \quad |P_\lambda v_1(t) - P_\lambda v_2(t)| \rightarrow 0 \quad \text{as } t \rightarrow \infty$$

imply that

$$\|v_1(t) - v_2(t)\| \rightarrow 0 \quad \text{as } t \rightarrow \infty.$$

Before proceeding, let us first note that a minor modification of the proof of Theorem 1.3 presented in [32] allows us to relax the hypothesis on  $g_1$  and  $g_2$ . In particular, it is sufficient to require in Theorem 1.3 that  $|Q_\lambda g_1(t) - Q_\lambda g_2(t)| \rightarrow 0$  as  $t \rightarrow \infty$ . The intuitive reason for this is clear. Since the difference of the low modes of  $v_1$  and  $v_2$  is already controlled by hypothesis and converge to zero, then all we need to show is that the difference of the high modes of  $v_1$  and  $v_2$  converge to zero. Therefore only the difference of the high modes of  $g_1$  and  $g_2$  need enter into the proof. In light of this observation, Theorem 1.3 may be rewritten as

**Theorem 1.4.** *Let  $v_1$  and  $v_2$  be two solutions of the two-dimensional Navier–Stokes equations on the  $L$ -periodic torus with corresponding forcing functions  $g_1$  and  $g_2$  and possibly different initial conditions. Then there exists a constant  $c_1$  independent of  $\nu$ ,  $L$ ,  $g_i$  or of any initial conditions such that for every  $\lambda(L/2\pi)^2 > c_1\text{Gr}(g_1)$  the limits*

$$|Q_\lambda g_1(t) - Q_\lambda g_2(t)| \rightarrow 0 \quad \text{and} \quad |P_\lambda v_1(t) - P_\lambda v_2(t)| \rightarrow 0 \quad \text{as } t \rightarrow \infty$$

imply

$$\|v_1(t) - v_2(t)\| \rightarrow 0 \quad \text{as } t \rightarrow \infty.$$

Thus, we may choose the low modes of  $g_1$  and  $g_2$  to be anything we like provided this choice ensures  $|P_\lambda v_1(t) - P_\lambda v_2(t)| \rightarrow 0$  as  $t \rightarrow \infty$ . In the case of continuous data assimilation we note that  $|Q_\lambda g_1(t) - Q_\lambda g_2(t)| = |Q_\lambda f_1(t) - Q_\lambda f_2(t)| = 0$  and  $|P_\lambda v_1(t) - P_\lambda v_2(t)| = |P_\lambda u_1(t) - P_\lambda u_2(t)| = 0$  for all time  $t \geq 0$ . Therefore, given  $\lambda > c_1\text{Gr}(f)$  and provided that the solution  $u_2(t)$  to (1.6) exists, it follows that  $\|u_1(t) - u_2(t)\| \rightarrow 0$  as  $t \rightarrow \infty$ . In particular, continuous data assimilation works for  $\lambda$  large enough.

We begin our study of how the convergence of  $u_2$  to  $u_1$  is affected by the spatial structure and length scales present in the forcing  $f$  by considering the time-independent forcing functions

$$\mathcal{G}(R) = \{ f : \text{Gr}(f) = R \}.$$

Given  $f \in \mathcal{G}(R)$  let  $u_1$  be the corresponding solution of (1.1). Rescale this solution as follows. Set  $\tilde{f}(x) = 8f(2x)$ ,  $\tilde{u}_1(x, t) = 2u_1(2x, 4t)$ ,  $\tilde{\pi}_1(x, t) = 4\pi_1(2x, 4t)$  and  $\tilde{u}_0(x) = 2u_0(2x)$ . Since  $\tilde{f}$ ,  $\tilde{u}_1$ ,  $\tilde{\pi}_1$  and  $\tilde{u}_0$  are  $L/2$ -periodic, then they are also  $L$ -periodic. Thus, we find that  $\tilde{u}_1$  satisfies

$$\frac{d\tilde{u}_1}{dt} + (\tilde{u}_1 \cdot \nabla)\tilde{u}_1 - \nu\Delta\tilde{u}_1 + \nabla\tilde{\pi}_1 = \tilde{f}, \quad \nabla \cdot \tilde{u}_1 = 0 \quad (1.8)$$

with initial conditions  $\tilde{u}_1(0) = \tilde{u}_0$  on the  $L$ -periodic torus. That is,  $\tilde{u}_1$  is a solution to the two-dimensional Navier–Stokes equations with forcing  $\tilde{f}$ . Since  $|\tilde{f}| = 8|f|$  then  $\tilde{f} \in \mathcal{G}(8R)$ . It follows that for every  $f \in \mathcal{G}(R)$  there is an  $\tilde{f} \in \mathcal{G}(8R)$  such that the corresponding solutions  $u_1$  and  $\tilde{u}_1$  have exactly the same dynamics.

The above observation shows that the Grashof number alone cannot determine the dynamical complexity of the two-dimensional Navier–Stokes equations. Therefore, in order to conduct a more detailed analysis we consider the negative Sobolev norm or dual norm of  $\|f\|$  defined as

$$\|f\|_* = L \left\{ \sum_{k \in \mathcal{J}} |k|^{-2} |\hat{f}_k|^2 \right\}^{1/2}. \quad (1.9)$$

As we shall see below, this norm will be useful in obtaining a determining modes result which distinguishes between forcing functions with the same Grashof number that are supported on different spatial length scales. Namely, we shall prove

**Theorem 1.5.** *Let  $u_1(t)$  be a solution on the global attractor of the two-dimensional Navier–Stokes equations (1.1) with time-independent forcing  $f \in L^2(\Omega)$ . Let  $u_2(t)$  be the approximation to  $u_1(t)$  obtained from the continuous data assimilation (1.6) of the observational measurements  $P_\lambda u_1(\tau)$  over the time interval  $\tau \in [0, t]$ . Then there are constants  $K_1$  and  $K_2$  independent of all initial conditions such that*

(i) *If there exists  $\alpha$  such that  $0 < 2\alpha \leq \nu\lambda - c_1^2\nu^{-3}\|f\|_*^2$  then*

$$|u_1(t) - u_2(t)| \leq |u_1(0) - u_2(0)| K_1 e^{-\alpha t} \quad \text{for } t \geq 0.$$

(ii) *If there exists  $\alpha$  such that  $0 < 2\alpha \leq \nu\lambda - c_1^2(\nu^3\lambda)^{-1}|f|^2$  then*

$$\|u_1(t) - u_2(t)\| \leq \|u_1(0) - u_2(0)\| K_2 e^{-\alpha t} \quad \text{for } t \geq 0.$$

Note that Theorem 1.5 shows that the convergence of  $u_2$  to  $u_1$  is, in fact, exponential in time. This leads us to the following definition.

**Definition 1.6.** The *rate of continuous data assimilation* of enstrophy is the supremum over all  $\alpha$  such that  $\|u_1(t) - u_2(t)\| = O(e^{-\alpha t})$  as  $t \rightarrow \infty$ .

This paper consists of analysis followed by computational results. First we place equations (1.1) and (1.6) in the appropriate functional settings that allow rigorous mathematical analysis of their solutions. We then state a number of important inequalities and facts that we shall need later on. The main goal of our work is to

demonstrate that there is a strong relationship between the spatial structure of  $f$ , the rate of continuous data assimilation and the number of determining modes in continuous data assimilation.

Our analysis begins by showing the continuous data assimilation equations (1.6) are globally well posed. For computational relevance we restrict our attention to strong solutions. We then establish a number of lemmas and eventually prove Theorem 1.5. We close with a discussion of whether the system of equations given by (1.1) and (1.6) is dissipative. When  $\lambda = 0$  equation this system is dissipative since in this case  $f_2 = f$  and the feedback term  $P_\lambda\{(u_2 \cdot \nabla)u_2 - (u_1 \cdot \nabla)u_1\} = 0$ . Thus  $u_2$  is a solution of the two-dimensional Navier–Stokes equations for forcing  $f$ . For

$$\lambda > \min \{c_1^2 \nu^{-4} \|f\|_*^2, c_1 \nu^{-2} |f|\} \quad (1.10)$$

dissipativity follows from the convergence of  $u_2$  to  $u_1$  as in Theorem 1.5. However, for intermediate values of  $\lambda$  the dissipativity of the continuous data assimilation equations remains in question.

Our computational results consist of two sets of experiments. All experiments were performed with  $\nu = 0.0001$  and  $\eta = Q_\lambda u_2(0) = 0$  on the  $2\pi$ -periodic torus for forcing functions with a Grashof number of  $R = 250000$ . Guided by Theorem 1.5 we first consider time-independent forcing functions  $f \in \mathcal{G}(R)$  supported on an annulus in Fourier space. Thus,  $f$  may be written

$$f = \sum_{\lambda_m \leq k^2 \leq \lambda_M} \hat{f}_k \phi_k. \quad (1.11)$$

with  $\hat{f}_k = \overline{\hat{f}_{-k}}$ ,  $k \cdot \hat{f}_k = 0$  and  $\hat{f}_0 = 0$ . We take the width of the annulus to be

$$\lambda_M - \lambda_m = 4\lambda_f^{1/2} - 2 \quad \text{where} \quad \lambda_f = (\lambda_m + \lambda_M)/2.$$

The width of the annulus is proportional to the wave number about which it is centered. It was shown by Constantin, Foias and Manley in [10] that no Kolmogorov flow, that is no flow driven by forcing only one Fourier mode, can sustain a Kraichnan inertial range spectrum in a statistically steady state. However, two eigenmodes can be sufficient. When  $\lambda_f \geq 1$  our condition ensures that  $f$  forces Fourier modes over a range of different eigenvalues. In particular, these forcing functions generate nonlinear interactions leading to time-dependent flows involving all the Fourier modes. This avoids the forcing functions exhibited by Marchioro in [37] which lead to steady flows which are globally asymptotically stable for any Reynolds number. In particular, Marchioro obtains

**Theorem 1.7.** *If  $f$  is supported on only the lowest modes in Fourier space then the solution to (2.6) converges to a steady flow which is globally asymptotically stable.*

Constantin, Foias and Temam give a simplified proof of this result in [11].

For any given  $\lambda_f$  let  $\mathcal{F}(\lambda_f)$  be the set of all functions  $f$  of the form (1.11) such that  $\text{Gr}(f) = R$ . In this way we obtain a one parameter family of subsets  $\mathcal{F}(\lambda_f)$  of

$\mathcal{G}(R)$  such that each subset consists of functions supported only on certain specified spatial length scales. For functions  $f \in \mathcal{F}(\lambda_f)$  we have that

$$(\lambda_f^{1/2} + 1)^{-2} |f|^2 \leq \|f\|_*^2 \leq (\lambda_f^{1/2} - 1)^{-2} |f|^2. \quad (1.12)$$

Therefore,  $\|f\|_*$  decreases for  $f \in \mathcal{F}(\lambda_f)$  as  $\lambda_f$  increases.

In our first set of experiments we vary  $\lambda_f$  from 25 through 625 and select functions  $f \in \mathcal{F}(\lambda_f)$  by choosing the amplitudes of the coefficients  $\hat{f}_k$  in (1.11) according to a Gaussian distribution. For each function selected, a number of continuous data assimilation experiments were conducted using different values of  $\lambda$  for the observational measurements  $P_\lambda u_1(t)$ . We measure how the rate of continuous data assimilation  $\alpha$  depends on the data assimilation parameter  $\lambda$  and the forcing length-scale parameter  $\lambda_f$ . For each forcing function  $f$ , the number of determining modes is consequently the rank of the smallest projection  $P_\lambda$  for which  $\alpha$  is clearly positive.

**Table 1.** The relationship between length scale  $\lambda_f$  in the forcing,  $\lambda_c$  and the number of determining modes  $N_c$ .

$\lambda_f$	25	64	121	169	256	361	484	529	576	625
$\lambda_c$	4	13	26	49	73	82	73	65	27	10
$N_c$	12	44	88	148	232	260	232	212	88	36

The results in the first half of Table 1 are, at first, rather surprising. The analytical bounds in part (i) of Theorem 1.5 suggest that the number of determining modes should decrease as  $\lambda_f$  increases; however, our computations indicate that the number of determining modes actually increases by more than an order of magnitude while  $\lambda_f$  ranges from 25 to 361. Only for  $\lambda_f$  greater than 361 does the number of determining modes given by our calculations reflect the decrease of  $\|f\|_*$  as  $\lambda_f$  increases.

Why does a flow driven by a function in  $\mathcal{F}(428)$  require more determining modes than a flow driven by a function in  $\mathcal{F}(25)$ ? We conduct a second set of computational experiments to shed some light on the cause of this phenomenon. Given  $f_L \in \mathcal{F}(25)$  and  $f_H \in \mathcal{F}(484)$  we set  $f = \theta_L f_L + \theta_H f_H$  where  $\theta_L^2 + \theta_H^2 = 1$ . In this way we obtain forcing functions supported on two disjoint annuli in Fourier space—one on small wave numbers, the other on large. Here  $\theta_L$  and  $\theta_H$  are parameters determining the relative weights of the large and small length scales in the forcing. When  $\theta_H$  is close to zero  $f$  may be viewed as the perturbation of the large scales  $f_L$  by the small scales  $f_H$ ; when  $\theta_L$  is close to zero  $f$  is the perturbation of the small scales  $f_H$  by the large scales  $f_L$ . We determine which perturbation more significantly affects the number of determining modes computationally in Table 2.



**Table 2.** The relationship between the weights  $\theta_L$  and  $\theta_H$  in the forcing,  $\lambda_c$  and the number of determining modes  $N_c$ .

$\theta_L$	0	0.080	0.160	0.320	0.768	1
$\theta_H$	1	0.997	0.987	0.947	0.640	0
$\lambda_c$	73	37	26	13	5	4
$N_c$	232	120	88	44	20	12

As shown by the first three columns, perturbing the small scales by the large scales has the greatest effect. This suggests that it is the absence of an increasing number of the large length scales in the forcing which is primarily responsible for the increase in number of determining modes as  $\lambda_f$  ranging from 25 though 361 in the first set of experiments.

We dedicate this paper to the memory of Oscar P. Manley, a good friend and source of encouragement, whose interest and physical insight motivated and laid the foundations for our work.

## 2. Preliminaries

In this section we characterize the spaces  $H$ ,  $V$  and  $V'$  which appear in the study of the Navier–Stokes equations and state a number of inequalities and facts that we shall need later on. For further details see, for example, Constantin and Foias [9], Doering and Gibbon [16], Robinson [39] or Temam [40, 41].

First, define the spaces  $V_\alpha$  in terms of the formal Fourier series (1.2) as

$$V_\alpha = \left\{ u = \sum_{k \in \mathcal{J}} \hat{u}_k \phi_k : \|u\|_\alpha^2 < \infty, \quad \hat{u}_k = \overline{\hat{u}_{-k}}, \quad k \cdot \hat{u}_k = 0 \quad \text{and} \quad \hat{u}_0 = 0 \right\}$$

where the norm

$$\|u\|_\alpha^2 = L^2 \sum_{k \in \mathcal{J}} |k|^{2\alpha} |\hat{u}_k|^2. \quad (2.1)$$

Note that

$$\|u\|_\alpha = \sup \{ \langle u, v \rangle : v \in V_{-\alpha} \quad \text{and} \quad \|v\|_{-\alpha} = 1 \} \quad (2.2)$$

where the pairing

$$\langle u, v \rangle = L^2 \sum_{k \in \mathcal{J}} \hat{u}_k \cdot \hat{v}_{-k}.$$

Fourier theory implies that  $V_\alpha$  is a subspace of  $L^2(\Omega)$  for  $\alpha \geq 0$ . Furthermore,  $V_{-\alpha}$  may be identified with the continuous dual of  $V_\alpha$ .

A relation exists between the norms defined in (2.1) and the projections defined in (1.4) which allows us to bound the norms of  $Q_\lambda u$  and  $P_\lambda u$  in a way that depends on the resolution parameter  $\lambda$ . For  $\alpha < \beta$  we obtain the following version of the Poincaré inequality

$$\|Q_\lambda u\|_\alpha^2 = L^2 \sum_{|k|^2 > \lambda} |k|^{2\alpha} |\hat{u}_k|^2 \leq \frac{L^2}{\lambda^{\beta-\alpha}} \sum_{|k|^2 > \lambda} |k|^{2\beta} |\hat{u}_k|^2 = \frac{1}{\lambda^{\beta-\alpha}} \|Q_\lambda u\|_\beta^2, \quad (2.3)$$

and for  $\alpha > \beta$  we obtain the inequality

$$\|P_\lambda u\|_\alpha^2 = L^2 \sum_{|k|^2 \leq \lambda} |k|^{2\alpha} |\hat{u}_k|^2 \leq L^2 \lambda^{\alpha-\beta} \sum_{|k|^2 \leq \lambda} |k|^{2\beta} |\hat{u}_k|^2 = \lambda^{\alpha-\beta} \|P_\lambda u\|_\beta^2. \quad (2.4)$$

Since  $Q_{\lambda_1} u = u$  for  $\lambda_1 = (2\pi/L)^2$  then (2.3) yields the usual Poincaré inequality

$$\|u\|_\alpha^2 \leq \frac{1}{\lambda_1^{\beta-\alpha}} \|u\|_\beta^2 \quad \text{for} \quad \alpha < \beta. \quad (2.5)$$

The functional spaces for solving (1.1) and (1.6) may now be defined as  $H = V_0$ ,  $V = V_1$  and  $V' = V_{-1}$ . Note that the norms  $\|u\|_0$ ,  $\|u\|_1$  and  $\|u\|_{-1}$  are respectively the norms  $|u|$ ,  $\|u\|$  and  $\|u\|_*$  given in (1.3) and (1.9). Thus,  $H$  consists of the square-integrable functions on the  $L$ -periodic torus  $\Omega$  which are divergence free and have zero mean,  $V$  are those functions in  $H$  whose first order derivatives are also square integrable, and  $V'$  is the dual of  $V$ . Moreover, by Parseval's identity the norms on  $H$  and  $V$  may also be expressed as  $|u| = \left\{ \int_\Omega u \cdot u \right\}^{1/2}$  and  $\|u\| = |\nabla u| = |\nabla \times u|$ .

**Definition 2.1.** Define the Leray projector  $P_\sigma: L^2 \rightarrow H$  to be the  $L^2$  orthogonal projection from  $L^2$  onto  $H$ . Further define  $A: V \rightarrow V'$  and  $B: V \times V \rightarrow V'$  to be the continuous extensions of the operators given by

$$Au = -P_\sigma \Delta u \quad \text{and} \quad B(u, v) = P_\sigma(u \cdot \nabla v)$$

for any suitably smooth function  $u$ . Notice that the domain  $D(A)$  of  $A$  is  $V_2$ .

For  $u_0 \in V$  and  $f \in H$  we write the Navier–Stokes equations (1.1) as the functional equation in  $H$  given by

$$\frac{du_1}{dt} + \nu Au_1 + B(u_1, u_1) = f \quad (2.6)$$

with initial conditions  $u_1(0) = u_0$ . Under these hypothesis equations (2.6) possess unique strong solutions depending continuously on the initial condition  $u_0$ . This is stated specifically as

**Theorem 2.2.** *Let  $u_0 \in V$  and  $f \in L_{\text{loc}}^2((0, \infty); H)$ . Then (2.6) has unique strong solutions that satisfy*

$$u_1 \in L^\infty((0, T); V) \cap L^2((0, T); D(A)) \quad \text{and} \quad \frac{du_1}{dt} \in L^2((0, T); H)$$

for any  $T > 0$ . Furthermore, this solution is in  $C([0, T]; V)$  and depends continuously on the initial data  $u_0$  in the  $V$  norm.

A proof of this theorem can be found, for example, in any of the references [9], [16], [39] or [40, 41] mentioned above. In the next section we prove a similar result for the continuous data assimilation equations (1.6) governing the evolution of  $u_2(t)$ . Note that the main difficulty there lies in controlling the feedback forcing  $f_2$ .

Let us now recall some algebraic properties of the non-linear term  $B(u, v)$  that play an important role in our analysis. These results may be found in any of the references [9], [16], [39] or [40, 41]. For  $u, v, w \in V$  we have that

$$\langle B(u, v), w \rangle = -\langle B(u, w), v \rangle \quad (2.7)$$

and consequently

$$\langle B(u, v), v \rangle = 0. \quad (2.8)$$

Furthermore, if  $v \in D(A)$  then

$$(B(v, v), Av) = 0 \quad (2.9)$$

and by differentiation of (2.9) we obtain

$$(B(u, v), Av) + (B(v, u), Av) + (B(v, v), Au) = 0 \quad (2.10)$$

for  $u, v \in D(A)$ . Note that conditions (2.9) and (2.10) are valid only for the two-dimensional Navier–Stokes equations on a periodic domain.

The non-linear term may be estimated by Hölder’s inequality followed by Ladyzhenskaya’s inequality [34]. In order to explicitly estimate the constants appearing in our analysis we state Ladyzhenskaya’s inequality here as

**Lemma 2.3.** Given  $u \in V$  then

$$\|u\|_{L^4}^2 \leq c_1 \|u\| \|u\| \quad (2.11)$$

where  $c_1 \leq 2 + (2\pi)^{-1}$  for the two-dimensional torus  $\Omega$ .

With this result in hand, if  $u, v, w \in V$  then

$$|\langle B(u, v), w \rangle| \leq \|u\|_{L^4} \|v\| \|w\|_{L^4} \leq c_1 |u|^{1/2} \|u\|^{1/2} \|v\| |w|^{1/2} \|w\|^{1/2}, \quad (2.12)$$

and if  $u \in V, v \in D(A)$  and  $w \in H$  then

$$|\langle B(u, v), w \rangle| \leq \|u\|_{L^4} \|\nabla v\|_{L^4} |w| \leq c_1 |u|^{1/2} \|u\|^{1/2} \|v\|^{1/2} |Av|^{1/2} |w|. \quad (2.13)$$

We end this section with some well known bounds on the time averages of  $\|u_1\|$  and  $|Au_1|$  in terms of  $u_0$  and  $f$  which will be used in the next section.

**Lemma 2.4.** *Let  $u_1(t)$  be the unique strong solution to (2.6) with time-dependent forcing  $f \in L^2_{\text{loc}}((0, \infty); H)$  and initial condition  $u_0 \in V$ . Then*

$$\frac{1}{t} \int_0^t \|u_1(\tau)\|^2 d\tau \leq \frac{1}{\nu t} |u_0|^2 + \frac{1}{\nu^2 t} \int_0^t \|f(\tau)\|_*^2 d\tau \quad (2.14)$$

and

$$\frac{1}{t} \int_0^t |Au_1(\tau)|^2 d\tau \leq \frac{1}{\nu t} \|u_0\|^2 + \frac{1}{\nu^2 t} \int_0^t |f(\tau)|^2 d\tau. \quad (2.15)$$

**Proof:** The proof may be found in any of the references [9], [16], [39] or [40, 41]. For completeness, we shall present formal calculation here that could be made rigorous if so desired.

To derive the first inequality, multiply (2.6) by  $u_1$  and use (2.8) to obtain

$$\frac{1}{2} \frac{d}{dt} |u_1|^2 + \nu \|u_1\|^2 = (f, u_1) \leq \|f\|_* \|u_1\|.$$

Note that since  $u_1 \in V$  and  $f \in H \subseteq V'$  we may view  $f$  as an element of  $V'$  and estimate  $(f, u_1)$  by  $\|f\|_* \|u_1\|$ . Applying Young's inequality gives

$$\frac{d}{dt} |u_1|^2 + \nu \|u_1\|^2 \leq \frac{1}{\nu} \|f\|_*^2 \quad (2.16)$$

which upon integrating in time yields

$$|u_1(t)|^2 + \nu \int_0^t \|u_1(\tau)\|^2 d\tau \leq |u_0|^2 + \frac{1}{\nu} \int_0^t \|f(\tau)\|_*^2 d\tau.$$

After dropping the first term on the left, inequality (2.14) follows.

To derive the second inequality, multiply (2.6) by  $Au_1$  and use (2.9) to obtain

$$\frac{1}{2} \frac{d}{dt} \|u_1\|^2 + \nu |Au_1|^2 = (f, Au_1).$$

Applying Cauchy–Schwarz and Young's inequalities gives

$$\frac{d}{dt} \|u_1\|^2 + \nu |Au_1|^2 \leq \frac{1}{\nu} |f|^2 \quad (2.17)$$

which upon integrating in time yields

$$\|u_1(t)\|^2 + \nu \int_0^t |Au_1(\tau)|^2 d\tau \leq \|u_0\|^2 + \frac{1}{\nu} \int_0^t |f(\tau)|^2 d\tau.$$

After dropping the first term on the left, inequality (2.15) follows.  $\square$

### 3. Analytical Results for Continuous Data Assimilation

We treat the continuous data assimilation equations (1.6) as a functional differential equation in the same way that the Navier–Stokes equations (1.1) were treated in the previous section to obtain (2.6) to arrive at the coupled system

$$\begin{cases} \frac{du_1}{dt} + \nu Au_1 + B(u_1, u_1) = f \\ \frac{du_2}{dt} + \nu Au_2 + B(u_2, u_2) = f + P_\lambda (B(u_2, u_2) - B(u_1, u_1)) \end{cases} \quad (3.1)$$

with initial conditions  $u_1(0) = u_0$  and  $u_2(0) = P_\lambda u_0 + \eta$  where  $u_0 \in V$  and  $\eta \in Q_\lambda V$ .

The solution to equation (3.1) may be viewed as two solutions  $u_1$  and  $u_2$  to the Navier–Stokes equations (2.6) with corresponding forcing  $f_1$  and  $f_2$  given by

$$f_1 = f \quad \text{and} \quad f_2 = f + P_\lambda(B(u_2, u_2) - B(u_1, u_1)). \quad (3.2)$$

Note that the forcing function  $f_2$  as defined above is actually the projection with respect to  $P_\sigma$  of the function defined by (1.7) in the introduction. Since  $f_2$  is chosen in a complicated way depending on a feedback with  $u_2$ , it is not immediately clear that the second equation in (3.1) is globally well posed. This issue is settled by

**Theorem 3.1.** *Let  $T > 0$  and  $\lambda \geq 0$ . If  $u_0 = u_1(0) \in V$ ,  $\eta = Q_\lambda u_2(0) \in Q_\lambda V$  and  $f \in L^2_{\text{loc}}((0, \infty); H)$  then (3.1) viewed as a system of functional equations in  $H$  has a unique strong solution that satisfies*

$$u_i \in L^\infty((0, T); V) \cap L^2((0, T); D(A)) \quad \text{and} \quad \frac{du_i}{dt} \in L^2((0, T); H) \quad (3.3)$$

for  $i = 1, 2$ . Furthermore, the solutions are in  $C([0, T]; V)$  and depend continuously on the initial data  $u_0$  and  $\eta$  in the  $V$  norm.

**Proof:** First we show existence of solutions. For  $u_1$  this result follows from the classical theory of the Navier–Stokes equations given by Theorem 2.2. For  $u_2$  we use the Galerkin method. Let  $P_n$  be the  $n$ -th Galerkin projector and assume that  $n$  is large enough that  $P_\lambda H \subseteq P_n H$ . The solution  $u_2^n$  to the finite-dimensional Galerkin truncation of the second equation in (3.1) satisfies

$$\frac{du_2^n}{dt} + \nu A u_2^n + P_n B(u_2^n, u_2^n) = P_n f + P_\lambda(B(u_2^n, u_2^n) - B(u_1, u_1)). \quad (3.4)$$

Solutions to this ordinary differential equation exist for short times since the non-linearity is locally Lipschitz. Long time existence follows from the estimates we will provide shortly. Moreover, since these estimates are uniform in  $n$ , the compactness theorems of Aubin [1] can be used to extract subsequences as  $n \rightarrow \infty$  in such a way that  $u_2^n$  converges to a solution to (3.1) satisfying (3.3). Further details may be found, for example, in [9], [16], [39], or [40, 41]. As these techniques are well known, we shall content ourselves here with a formal calculation that could be made rigorous if so desired.

In the estimates that follow, we denote the Galerkin solution  $u_2^n$  to (3.4) by  $u_2$  for notational simplicity. Since  $u_1 \in C([0, T]; V)$  then there exists  $M_1$  large enough that  $\|u_1(t)\| \leq M_1$  for all  $t$ . The low modes  $P_\lambda u_2(t)$  are bounded in any norm since all finite dimensional norms are equivalent and  $P_\lambda u_2(t) = P_\lambda u_1(t)$ . In particular, the Poincaré inequality (2.4) implies that

$$|AP_\lambda u_2(t)| = |AP_\lambda u_1(t)| \leq \lambda^{1/2} \|P_\lambda u_1(t)\| \leq \lambda^{1/2} \|u_1(t)\| \leq \lambda^{1/2} M_1. \quad (3.5)$$

In the case that  $f$  is time independent then there are uniform estimates on  $|Au_1(t)|$  for  $u_1$  on the attractor, see, for example [9], [16], [39], or [40, 41]. In this case we could bound  $|AP_\lambda u_2(t)|$  independently of  $\lambda$ .

Estimate the high modes  $Q_\lambda u_2(t)$  by taking the inner products of (3.4) with  $AQ_\lambda u_2$  to obtain

$$\frac{1}{2} \frac{d}{dt} \|Q_\lambda u_2\|^2 + \nu |AQ_\lambda u_2|^2 = (f, AQ_\lambda u_2) - (B(u_2, u_2), AQ_\lambda u_2). \quad (3.6)$$

The first term on the right side may be estimated using Cauchy–Schwarz and Young’s inequalities as

$$(f, AQ_\lambda u_2) \leq \frac{2}{\nu} |f|^2 + \frac{\nu}{8} |AQ_\lambda u_2|^2.$$

To estimate the second term use (2.9) and the bi-linearity repeatedly to obtain

$$\begin{aligned} -(B(u_2, u_2), AQ_\lambda u_2) &= (B(u_2, u_2), AP_\lambda u_2) \\ &= (B(P_\lambda u_2, u_2), AP_\lambda u_2) + (B(Q_\lambda u_2, u_2), AP_\lambda u_2) \\ &= (B(Q_\lambda u_2, P_\lambda u_2), AP_\lambda u_2) \\ &\quad + (B(P_\lambda u_2, Q_\lambda u_2), AP_\lambda u_2) + (B(Q_\lambda u_2, Q_\lambda u_2), AP_\lambda u_2). \end{aligned}$$

Now (2.13) and (2.3) followed by Young’s inequality and then (3.5) yields

$$\begin{aligned} |(B(Q_\lambda u_2, P_\lambda u_2), AP_\lambda u_2)| &\leq c_1 |Q_\lambda u_2|^{1/2} \|Q_\lambda u_2\|^{1/2} \|P_\lambda u_2\|^{1/2} |AP_\lambda u_2|^{3/2} \\ &\leq c_1 \lambda^{-3/4} |AQ_\lambda u_2| \|P_\lambda u_2\|^{1/2} |AP_\lambda u_2|^{3/2} \\ &\leq \frac{2c_1^2}{\nu \lambda^{3/2}} \|P_\lambda u_2\| \|AP_\lambda u_2\|^3 + \frac{\nu}{8} |AQ_\lambda u_2|^2 \\ &\leq \frac{2c_1^2 M_1^4}{\nu} + \frac{\nu}{8} |AQ_\lambda u_2|^2. \end{aligned}$$

The inequalities (2.13), (2.3) and (2.5) followed by Young’s inequality and (3.5) yields

$$\begin{aligned} |(B(P_\lambda u_2, Q_\lambda u_2), AP_\lambda u_2)| &\leq c_1 |P_\lambda u_2|^{1/2} \|P_\lambda u_2\|^{1/2} \|Q_\lambda u_2\|^{1/2} |AQ_\lambda u_2|^{1/2} |AP_\lambda u_2| \\ &\leq c_1 \lambda^{-1/4} |P_\lambda u_2|^{1/2} \|P_\lambda u_2\|^{1/2} |AP_\lambda u_2| |AQ_\lambda u_2| \\ &\leq c_1 \lambda^{-1/4} \lambda_1^{-1/4} \|P_\lambda u_2\| \|AP_\lambda u_2\| |AQ_\lambda u_2| \\ &\leq \frac{2c_1^2}{\nu \lambda^{1/2} \lambda_1^{1/2}} \|P_\lambda u_2\|^2 |AP_\lambda u_2|^2 + \frac{\nu}{8} |AQ_\lambda u_2|^2 \\ &\leq \left( \frac{2c_1^2 M_1^4}{\nu} \right) \frac{\lambda^{1/2}}{\lambda_1^{1/2}} + \frac{\nu}{8} |AQ_\lambda u_2|^2. \end{aligned}$$

Finally (2.13) and (2.3) followed by Young’s inequality and (3.5) yields

$$\begin{aligned} |(B(Q_\lambda u_2, Q_\lambda u_2), AP_\lambda u_2)| &\leq c_1 |Q_\lambda u_2|^{1/2} \|Q_\lambda u_2\| |AQ_\lambda u_2|^{1/2} |AP_\lambda u_2| \\ &\leq c_1 \lambda^{-1/2} \|Q_\lambda u_2\| |AQ_\lambda u_2| |AP_\lambda u_2| \\ &\leq \frac{2c_1^2}{\nu \lambda} \|Q_\lambda u_2\|^2 |AP_\lambda u_2|^2 + \frac{\nu}{8} |AQ_\lambda u_2|^2 \\ &\leq \frac{2c_1^2 M_1^2}{\nu} \|Q_\lambda u_2\|^2 + \frac{\nu}{8} |AQ_\lambda u_2|^2. \end{aligned}$$

It follows that (3.6) becomes

$$\frac{d}{dt}\|Q_\lambda u_2\|^2 + \nu|AQ_\lambda u_2|^2 \leq \frac{2c_1^2 M_1^2}{\nu}\|Q_\lambda u_2\|^2 + \frac{4}{\nu}|f|^2 + \beta_1 \quad (3.7)$$

where the constant

$$\beta_1 = \frac{2c_1^2 M_1^4}{\nu} \left\{ 1 + \frac{\lambda^{1/2}}{\lambda_1^{1/2}} \right\}.$$

Applying (2.3) to the second term on the left of (3.7) and regrouping yields

$$\frac{d}{dt}\|Q_\lambda u_2\|^2 + \left\{ \nu\lambda - \frac{2c_1^2 M_1^2}{\nu} \right\} \|Q_\lambda u_2\|^2 \leq \frac{4}{\nu}|f|^2 + \beta_1.$$

This inequality may be written

$$\frac{d\xi}{dt} + \beta_2 \xi \leq \frac{4}{\nu}|f|^2 + \beta_1 \quad (3.8)$$

where

$$\beta_2 = \nu\lambda - \frac{2c_1^2 M_1^2}{\nu} \quad \text{and} \quad \xi = \|Q_\lambda u_2\|^2.$$

Gronwall's inequality applied to (3.8) yields that

$$\xi(t) \leq \xi(0)e^{-\beta_2 t} + \frac{\beta_1}{\beta_2}(1 - e^{-\beta_2 t}) + \frac{4}{\nu} \int_0^t |f(s)|^2 e^{-\beta_2(t-s)} ds. \quad (3.9)$$

Since  $f \in L^2_{\text{loc}}((0, \infty); H)$  it follows that  $\|Q_\lambda u_2(t)\|^2$  is bounded for any interval  $[0, T]$ . Hence  $u_2 \in L^\infty((0, T); V)$ .

Next we show  $u_2 \in L^2((0, T); D(A))$ . Let  $M_2$  be the bound exhibited above such that  $\|u_2(t)\|^2 \leq M_2$  for all  $t$  in  $[0, T]$ . Substituting this bound into (3.7) obtains

$$\frac{d}{dt}\|Q_\lambda u_2\|^2 + \nu|AQ_\lambda u_2|^2 \leq \frac{4}{\nu}|f|^2 + \beta_3 \quad (3.10)$$

where

$$\beta_3 = \frac{2c_1^2 M_1^2 M_2^2}{\nu} + \beta_1.$$

Gronwall's inequality applied to (3.10) yields

$$\|Q_\lambda u_2(T)\|^2 + \nu \int_0^T |AQ_\lambda u_2|^2 \leq \|Q_\lambda u_2(0)\|^2 + \frac{4}{\nu} \int_0^T |f|^2 + T\beta_3.$$

Upon dropping the first term on the left and majorizing the first term on the right by  $M_2^2$  it follows that

$$\int_0^T |AQ_\lambda u_2|^2 \leq \frac{1}{\nu} \left\{ M_2^2 + \frac{4}{\nu} \int_0^T |f|^2 + T\beta_3 \right\}.$$

Therefore  $u_2 \in L^2((0, T); D(A))$ .

The proof that  $du_2/dt \in L^2((0, T); H)$  proceeds in exactly the same way as for the two-dimensional Navier–Stokes equations. The Galerkin method then leads to the existence of solutions to (3.1) satisfying (3.3).

Next, we show that such solutions are unique and depend continuously on the initial data. Let  $u_i$  and  $v_i$  be two solutions to (3.1) satisfying (3.3) for  $i = 1, 2$  with initial conditions in  $V$  such that  $P_\lambda u_1(0) = P_\lambda u_2(0)$  and  $P_\lambda v_1(0) = P_\lambda v_2(0)$ . Let the constants  $M_1$  and  $M_2$  be chosen large enough so that  $\|u_i(t)\| \leq M_i$  and  $\|v_i(t)\| \leq M_i$  for  $i = 1, 2$  and almost every  $t$  in  $[0, T]$ . Let  $w_i = u_i - v_i$ . Since  $u_1$  and  $v_1$  are solutions to the standard two-dimensional Navier–Stokes equations, then Theorem 2.2 implies

$$\|w_1(t)\|^2 \leq \psi(t)\|w_1(0)\|^2 \quad \text{for } t \geq 0 \quad (3.11)$$

for some continuous monotone increasing function  $\psi(t)$  with  $\psi(0) = 1$ . To obtain similar estimates on  $w_2$ , subtract the equation for  $v_2$  from the equation for  $u_2$ . Thus,

$$\frac{dw_2}{dt} + \nu Aw_2 = P_\lambda(B(v_1, v_1) - B(u_1, u_1)) + Q_\lambda(B(v_2, v_2) - B(u_2, u_2)).$$

Introducing  $\mp P_\lambda B(v_1, u_1)$  and  $\mp P_\lambda B(v_2, u_2)$  on the right side yields

$$\frac{dw_2}{dt} + \nu Aw_2 = -P_\lambda(B(v_1, w_1) + B(w_1, u_1)) - Q_\lambda(B(v_2, w_2) + B(w_2, u_2)).$$

Since  $w_2 \in L^2(0, T; D(A))$  and  $dw_2/dt \in L^2(0, T; H)$  then the interpolation lemma of Lions–Magenes [36] implies that

$$\left(\frac{dw_2}{dt}, Aw_2\right) = \frac{1}{2} \frac{d}{dt} \|w_2\|^2.$$

See also Corollary 7.3 in [39] or Lemma 1.2 in [40]. Now, taking inner products with  $Aw_2$  and using the fact that  $P_\lambda w_2 = P_\lambda w_1$  we obtain

$$\begin{aligned} \frac{1}{2} \frac{d}{dt} \|w_2\|^2 + \nu |Aw_2|^2 &= -(B(v_1, w_1), P_\lambda Aw_1) - (B(w_1, u_1), P_\lambda Aw_1) \\ &\quad - (B(v_2, w_2), Q_\lambda Aw_2) - (B(w_2, u_2), Q_\lambda Aw_2). \end{aligned} \quad (3.12)$$

By (2.12), (2.4) and (2.5) and then (3.11) we have

$$\begin{aligned} |(B(v_1, w_1), P_\lambda Aw_1)| &\leq |v_1|^{1/2} \|v_1\|^{1/2} \|w_1\| \|P_\lambda Aw_1\| \|P_\lambda Aw_1\| \\ &\leq \frac{\lambda^{3/2}}{\lambda_1^{1/2}} \|v_1\| \|w_1\|^2 \leq \frac{\lambda^{3/2}}{\lambda_1^{1/2}} M_1 \psi(t) \|w_1(0)\|^2. \end{aligned}$$

Similarly we estimate

$$\begin{aligned} |(B(w_1, u_1), P_\lambda Aw_1)| &\leq |w_1|^{1/2} \|w_1\|^{1/2} \|u_1\| \|P_\lambda Aw_1\| \|P_\lambda Aw_1\| \\ &\leq \frac{\lambda^{3/2}}{\lambda_1^{1/2}} \|u_1\| \|w_1\|^2 \leq \frac{\lambda^{3/2}}{\lambda_1^{1/2}} M_1 \psi(t) \|w_1(0)\|^2. \end{aligned}$$



Using (2.13), Young's inequality and then (2.5) we estimate

$$\begin{aligned}
|(B(v_2, w_2), Q_\lambda Aw_2)| &\leq |v_2|^{1/2} \|v_2\|^{1/2} \|w_2\|^{1/2} |Aw_2|^{3/2} \\
&\leq \left(\frac{3}{2\nu}\right)^3 \frac{1}{4} |v_2|^2 \|v_2\|^2 \|w_2\|^2 + \frac{\nu}{2} |Aw_2|^2 \\
&\leq \frac{27}{32\nu^3} \frac{M_2^4}{\lambda_1} \|w_2\|^2 + \frac{\nu}{2} |Aw_2|^2
\end{aligned}$$

and also

$$\begin{aligned}
|(B(w_2, u_2), Q_\lambda Aw_2)| &\leq |w_2|^{1/2} \|w_2\|^{1/2} \|u_2\|^{1/2} |Au_2|^{1/2} |Aw_2| \\
&\leq \frac{1}{2\nu} |w_2| \|w_2\| \|u_2\| |Au_2| + \frac{\nu}{2} |Aw_2|^2 \\
&\leq \frac{1}{2\nu} \lambda_1^{-1/2} \|w_2\|^2 \|u_2\| |Au_2| + \frac{\nu}{2} |Aw_2|^2 \\
&\leq \frac{1}{4\nu} \|w_2\|^2 \left\{ M_2^2 + \frac{1}{\lambda_1} |Au_2|^2 \right\} + \frac{\nu}{2} |Aw_2|^2.
\end{aligned}$$

Substituting these estimates into (3.12) we obtain

$$\frac{d}{dt} \|w_2\|^2 \leq \beta_4 \|w_1(0)\|^2 + \beta_5 \|w_2\|^2 \tag{3.13}$$

where

$$\beta_4(t) = 4 \frac{\lambda^{3/2}}{\lambda_1^{1/2}} M_1 \psi(t) \quad \text{and} \quad \beta_5(t) = \frac{1}{2\nu} \left\{ \frac{27M_2^4}{8\nu^2 \lambda_1} + M_2^2 + \frac{1}{\lambda_1} |Au_2(t)|^2 \right\}.$$

Gronwall's inequality applied to (3.13) yields that

$$\begin{aligned}
\|w_2(t)\|^2 &\leq \|w_2(0)\|^2 \exp \left\{ \int_0^t \beta_5(s) ds \right\} \\
&\quad + \|w_1(0)\|^2 \int_0^t \beta_4(\tau) \exp \left\{ \int_\tau^t \beta_5(s) ds \right\} d\tau.
\end{aligned}$$

Since  $u_2 \in L^2((0, T); D(A))$  then continuity with respect to the initial conditions follows. In particular, solutions of (3.1) satisfying (3.3) are unique.  $\square$

Note that the bounds in (3.9) are not uniform in time unless  $\beta_2 > 0$ . This implies that  $\lambda$  must be sufficiently large for us to prove that the system (3.1) is dissipative. A slightly sharper result than the one which results from the above observation appears as Theorem 3.5 at the end of this section.

The uniqueness given by Theorem 3.1 guarantees that if  $u_1(t)$  and  $u_2(t)$  happen to agree at some point in time, then they will remain equal for all subsequent times. In particular, if  $\eta = Q_\lambda u_0$  then  $u_1(t) = u_2(t)$  for all  $t$ . The following lemma establishes bounds on the convergence of continuous data assimilation in terms of time averages

of the reference calculation  $u_1$ . As  $\lambda$  increases, the resolution of the measurements becomes finer. Therefore, we expect that  $u_2(t)$  becomes a better and better approximation of  $u_1(t)$  as  $\lambda \rightarrow \infty$ .

**Lemma 3.2.** *Let  $u_1(t)$  and  $u_2(t)$  be the unique strong solutions to (3.1) with  $u_0 = u_1(0) \in V$ ,  $\eta = Q_\lambda u_2(0) \in Q_\lambda V$  and  $f \in L^2_{\text{loc}}((0, \infty); H)$  given by Theorem 3.1. Then*

$$|u_1(t) - u_2(t)|^2 \leq |u_1(0) - u_2(0)|^2 \exp \left\{ -\nu\lambda t + \frac{c_1^2}{\nu} \int_0^t \|u_1(\tau)\|^2 d\tau \right\} \quad (3.14)$$

and

$$\|u_1(t) - u_2(t)\|^2 \leq \|u_1(0) - u_2(0)\|^2 \exp \left\{ -\nu\lambda t + \frac{c_1^2}{\nu\lambda} \int_0^t |Au_1(\tau)|^2 d\tau \right\}. \quad (3.15)$$

**Proof:** Let  $\delta = u_1 - u_2$ . Subtract the second equation in (3.1) from the first to obtain

$$\frac{d\delta}{dt} + \nu A\delta + Q_\lambda (B(u_1, u_1) - B(u_2, u_2)) = 0. \quad (3.16)$$

Introduce  $\mp Q_\lambda B(u_2, u_1)$  and further introduce  $\pm Q_\lambda B(u_1, \delta)$  into (3.16) to obtain

$$\frac{d\delta}{dt} + \nu A\delta + Q_\lambda (B(\delta, u_1) + B(u_1, \delta) - B(\delta, \delta)) = 0. \quad (3.17)$$

We shall make two estimates showing the convergence of  $\delta$  to zero. First, we find conditions under which  $|\delta(t)| \rightarrow 0$  as  $t \rightarrow \infty$ , and second, we find conditions under which  $\|\delta(t)\| \rightarrow 0$  as  $t \rightarrow \infty$ .

We obtain estimates on  $|\delta|$  by multiplying (3.17) by  $\delta$  and integrating. Since  $Q_\lambda \delta = \delta$  it follows from (2.8) that

$$\frac{1}{2} \frac{d}{dt} |\delta|^2 + \nu \|\delta\|^2 + (B(\delta, u_1), \delta) = 0. \quad (3.18)$$

Inequality (2.12) followed by Young's inequality yields

$$|(B(\delta, u_1), \delta)| \leq c_1 |\delta| \|\delta\| \|u_1\| \leq \frac{c_1^2}{2\nu} |\delta|^2 \|u_1\|^2 + \frac{\nu}{2} \|\delta\|^2. \quad (3.19)$$

Substituting (3.19) into (3.18) obtains

$$\frac{d}{dt} |\delta|^2 + \nu \|\delta\|^2 \leq \frac{c_1^2}{\nu} |\delta|^2 \|u_1\|^2.$$

Applying (2.3) to the second term on the left yields

$$\frac{d}{dt} |\delta|^2 + \left\{ \nu\lambda - \frac{c_1^2}{\nu} \|u_1\|^2 \right\} |\delta|^2 \leq 0. \quad (3.20)$$

Now, Gronwall's inequality yields

$$|\delta(t)|^2 \leq |\delta(0)|^2 \exp \left\{ -\nu\lambda t + \frac{c_1^2}{\nu} \int_0^t \|u_1(\tau)\|^2 d\tau \right\}$$

Next, we obtain estimates on  $\|\delta\|$  by taking the  $L^2$  inner product of (3.17) with  $A\delta$ . Since  $Q_\lambda A\delta = A\delta$  it follows from (2.9) that

$$\frac{1}{2} \frac{d}{dt} \|\delta\|^2 + \nu |A\delta|^2 + (B(u_1, \delta), A\delta) + (B(\delta, u_1), A\delta) = 0.$$

Further applying (2.10) obtains

$$\frac{1}{2} \frac{d}{dt} \|\delta\|^2 + \nu |A\delta|^2 = (B(\delta, \delta), Au_1). \quad (3.21)$$

Estimate using (2.12) followed by (2.3) and then Young's inequality as

$$\begin{aligned} |(B(\delta, \delta), Au_1)| &\leq c_1 |\delta|^{1/2} \|\delta\| |A\delta|^{1/2} |Au_1| \\ &\leq c_1 \lambda^{-1/2} \|\delta\| |A\delta| |Au_1| \\ &\leq \frac{c_1^2}{2\nu\lambda} \|\delta\|^2 |Au_1|^2 + \frac{\nu}{2} |A\delta|^2. \end{aligned}$$

Then substitute this estimate into (3.21) to obtain

$$\frac{d}{dt} \|\delta\|^2 + \nu |A\delta|^2 \leq \frac{c_1^2}{\nu\lambda} \|\delta\|^2 |Au_1|^2.$$

Applying (2.3) to the second term on the left yields

$$\frac{d}{dt} \|\delta\|^2 + \left\{ \nu\lambda - \frac{c_1^2}{\nu\lambda} |Au_1|^2 \right\} \|\delta\|^2 \leq 0. \quad (3.22)$$

Now, Gronwall's inequality yields

$$\|\delta(t)\|^2 \leq \|\delta(0)\|^2 \exp \left\{ -\nu\lambda t + \frac{c_1^2}{\nu\lambda} \int_0^t |Au_1(\tau)|^2 d\tau \right\}.$$

This finishes the proof of the lemma.  $\square$

Combining Lemma 3.2 with Lemma 2.4 we obtain rigorous conditions on  $\lambda$  in terms of  $f$  and  $\nu$  which ensure that continuous data assimilation works. Namely, we prove the following version of Theorem 1.5.

**Theorem 3.3.** *Let*

$$M_1 = \left\{ \sup_{t>0} \frac{1}{t} \int_0^t \|f(\tau)\|_*^2 d\tau \right\}^{1/2} \quad \text{and} \quad M_2 = \left\{ \sup_{t>0} \frac{1}{t} \int_0^t |f(\tau)|^2 d\tau \right\}^{1/2}.$$

Then, given a bounded subset  $B_0 \subset V$  and  $f \in L^2_{\text{loc}}((0, T); H)$  with  $M_2 < \infty$ , there exists  $K_1$  and  $K_2$  large enough such that for every  $u_0 = u_1(0) \in B_0$  and  $\eta = Q_\lambda u_2(0) \in Q_\lambda V$  the solutions  $u_1(t)$  and  $u_2(t)$  to (3.1) satisfy

(i) If there exists  $\alpha$  such that  $0 < 2\alpha \leq \nu\lambda - c_1^2\nu^{-3}M_1^2$  then

$$|u_1(t) - u_2(t)| \leq |u_1(0) - u_2(0)|K_1e^{-\alpha t} \quad \text{for } t \geq 0.$$

(ii) If there exists  $\alpha$  such that  $0 < 2\alpha \leq \nu\lambda - c_1^2(\nu^3\lambda)^{-1}M_2^2$  then

$$\|u_1(t) - u_2(t)\| \leq \|u_1(0) - u_2(0)\|K_2e^{-\alpha t} \quad \text{for } t \geq 0.$$

**Proof:** Let  $\delta = u_1 - u_2$ . To estimate  $|\delta(t)|$  substitute (2.14) from Lemma 2.4 into (3.14) from Lemma 3.2 to obtain

$$\begin{aligned} |\delta(t)|^2 &\leq |\delta(0)|^2 \exp \left\{ -\nu\lambda t + \frac{tc_1^2}{\nu} \left( \frac{1}{\nu t} |u_0|^2 + \frac{1}{\nu^2} M_1^2 \right) \right\} \\ &\leq |\delta(0)|^2 \exp \left\{ \frac{c_1^2}{\nu^2} |u_0|^2 \right\} \exp \left\{ \left( -\nu\lambda + \frac{c_1^2}{\nu^3} M_1^2 \right) t \right\}. \end{aligned}$$

It follows that, if  $0 < 2\alpha \leq \nu\lambda - c_1^2\nu^{-3}M_1^2$  then  $|\delta(t)| \leq |\delta(0)|K_1e^{-\alpha t}$  where  $K_1$  is chosen large enough such that

$$K_1 \geq \exp \left\{ \frac{c_1^2}{2\nu^2} |u_0|^2 \right\} \quad \text{for all } u_0 \in B_0.$$

To estimate  $\|\delta(t)\|$  substitute (2.15) from Lemma 2.4 into (3.15) from Lemma 3.2 to obtain

$$\begin{aligned} \|\delta(t)\|^2 &\leq \|\delta(0)\|^2 \exp \left\{ -\nu\lambda t + \frac{tc_1^2}{\nu\lambda} \left( \frac{1}{\nu t} \|u_0\|^2 + \frac{1}{\nu^2} M_2^2 \right) \right\} \\ &\leq \|\delta(0)\|^2 \exp \left\{ \frac{c_1^2}{\nu^2\lambda} \|u_0\|^2 \right\} \exp \left\{ \left( -\nu\lambda + \frac{c_1^2}{\nu^3\lambda} M_2^2 \right) t \right\}. \end{aligned}$$

It follows that, if  $0 < 2\alpha \leq \nu\lambda - c_1^2(\nu^3\lambda)^{-1}M_2^2$  then  $\|\delta(t)\| \leq \|\delta(0)\|K_2e^{-\alpha t}$  where  $K_2$  is chosen large enough such that

$$K_2 \geq \exp \left\{ \frac{c_1^2}{2\nu^2\lambda} \|u_0\|^2 \right\} \quad \text{for all } u_0 \in B_0.$$

This finishes the proof.  $\square$

**Corollary 3.4.** *Under the hypothesis of Theorem 3.3 the approximation  $u_2$  converges to  $u_1$  in  $L^\infty([0, \infty]; V)$  as  $\lambda \rightarrow \infty$ .*

**Proof:** Since  $K_2$  in Theorem 3.3 may be chosen independently of  $\lambda$  then

$$\|u_1(t) - u_2(t)\| \leq \|u_1(0) - u_2(0)\|K_2e^{-\alpha t} \leq K_2\|Q_\lambda(u_0 - \eta)\| \rightarrow 0$$

as  $\lambda \rightarrow \infty$ . □

**Proof of Theorem 1.5.** Notice in the case  $f$  is time-independent that  $M_1 = \|f\|_*$  and  $M_2 = |f|$  in Theorem 3.3. The proof of Theorem 1.5 then follows from Theorem 3.3 and the fact that the global attractor of (2.6) is bounded in  $V$ . □

Note that any bounds on the critical value of  $\lambda$  for which continuous data assimilation works must remain invariant under the scaling presented in (1.8) in order to be sharp. Since all wave numbers in the original Fourier space are doubled upon setting  $\tilde{u}_1(x, t) = 2u_1(2x, 4t)$  and  $\tilde{f}(x) = 8f(2x)$ , then the observational measurements  $P_{\tilde{\lambda}}\tilde{u}_1(t)$  are equivalent to  $P_{\lambda}u_1(t)$  exactly when  $\tilde{\lambda} = 4\lambda$ .

Assume, first, that there is a bound on  $\lambda$  in terms of  $\|f\|_*$  which is sharp. In particular, suppose  $\lambda \sim C\|f\|_*^\beta$  for some constants  $C$  and  $\beta$ . Since  $\|\tilde{f}\|_* = 4\|f\|_*$  then rewriting  $\tilde{\lambda} \sim C\|\tilde{f}\|_*^\beta$  in terms of  $\lambda$  and  $f$  yields  $4\lambda \sim 4^\beta C|f|^\beta$ . It follows that  $\beta = 1$  and therefore  $\lambda \sim C\|f\|_*$ . However, the first bound in Theorem 3.3 depends on  $\|f\|_*^2$ , therefore it could not be sharp. Similarly, if  $\lambda \sim C|f|^\beta$ , then rescaling  $\tilde{\lambda} \sim C|\tilde{f}|^\beta$  yields  $4\lambda \sim C8^\beta|f|^\beta$ . It follows, in this case, that  $\beta = 2/3$  and so  $\lambda \sim C|f|^{2/3}$ . Thus, both of the results in Theorem 3.3 are only upper bounds.

We end this section with a result on the dissipativity of the continuous data assimilation equations (3.1). Whether this system of equations is dissipative for all, in particular smaller, values of  $\lambda$  appears to be an interesting open question.

**Theorem 3.5.** Given forcing  $f \in H$  and provided that  $\lambda$  satisfies (1.10), then the system of equations (3.1) is dissipative and has an absorbing ball in  $V$ .

**Proof:** Since  $u_1$  satisfies the usual two-dimensional Navier–Stokes equations with forcing  $f \in H$  then it has an absorbing ball in  $V$ . See, for example, [9], [16], [39] or [40, 41]. For  $u_2$  we use Theorem 3.3 to estimate  $f_2$  and use that estimate to find an absorbing ball.

Let  $\delta(t) = u_1(t) - u_2(t)$ . Then (2.4) implies

$$\begin{aligned} |f_1 - f_2| &\leq |P_\lambda B(u_2, u_2) - P_\lambda B(u_1, u_1)| \\ &\leq |P_\lambda B(\delta, \delta)| + |P_\lambda B(u_1, \delta)| + |P_\lambda B(\delta, u_1)| \\ &\leq \lambda^{3/2} \{ \|B(\delta, \delta)\|_{-3} + \|B(u_1, \delta)\|_{-3} + \|B(\delta, u_1)\|_{-3} \}. \end{aligned}$$

For  $w \in V_3$  the Sobolev embedding  $\|\nabla w\|_{L^\infty} \leq C\|w\|_3$  yields the estimates

$$\begin{aligned} |\langle B(\delta, \delta), w \rangle| &= |\langle B(\delta, w), \delta \rangle| \leq \|\nabla w\|_{L^\infty} |\delta|^2 \leq C\|w\|_3 |\delta|^2 \\ |\langle B(u_1, \delta), w \rangle| &= |\langle B(u_1, w), \delta \rangle| \leq \|\nabla w\|_{L^\infty} |u_1| |\delta| \leq C\|w\|_3 |u_1| |\delta| \\ |\langle B(\delta, u_1), w \rangle| &= |\langle B(\delta, w), u_1 \rangle| \leq \|\nabla w\|_{L^\infty} |u_1| |\delta| \leq C\|w\|_3 |u_1| |\delta|. \end{aligned}$$

If  $\lambda$  satisfies inequality (1.10) then Theorem 3.3 implies  $|\delta(t)| \rightarrow 0$  as  $t \rightarrow \infty$ . Thus,

$$|f_1 - f_2| \leq C\lambda^{3/2} \{ |\delta|^2 + 2|u_1||\delta| \} \rightarrow 0 \quad \text{as} \quad t \rightarrow \infty. \quad (3.23)$$

This implies that  $f_2$  has the same asymptotic bounds in time as  $f$ .

Now, Theorem 3.3 implies that for any bounded subset  $B_0 \subset V$  there exists a time  $s > 0$  such that for every  $u_0 \in B_0$  and  $\eta \in Q_\lambda V$  the corresponding  $f_2$  obeys

$$|f_2(t)| \leq 2|f| \quad \text{for} \quad t > s.$$

Let

$$B_1 = \{ u_2(s) : u_0 \in B_0 \quad \text{and} \quad \eta \in Q_\lambda B_0 \}.$$

Continuous dependence on the initial data given by Theorem 3.1 implies that  $B_1$  is bounded in  $V$ . Denote that bound by  $M_1$ . We now estimate  $\|u_2(t)\|$ .

Multiply the second equation in (3.1) by  $Au_2$  to obtain

$$\frac{1}{2} \frac{d}{dt} \|u_2\|^2 + \nu |Au_2|^2 = (f_2, Au_2).$$

Applying Cauchy-Schwarz and Young's inequalities gives

$$\frac{d}{dt} \|u_2\|^2 + \nu |Au_2|^2 = \frac{1}{\nu} |f_2|^2.$$

Applying the Poincaré inequality (2.5) to the second term on the right yields

$$\frac{d}{dt} \|u_2\|^2 + \nu \lambda_1 \|u_2\|^2 = \frac{1}{\nu} |f_2|^2$$

and integrating over the interval  $[s, t]$  obtains

$$\begin{aligned} \|u_2(t)\|^2 &\leq \|u_2(s)\|^2 e^{-\nu \lambda_1 (t-s)} + \frac{1}{\nu} \int_s^t e^{-\nu \lambda_1 (t-\tau)} |f_2(\tau)|^2 d\tau \\ &\leq M_1^2 e^{-\nu \lambda_1 (t-s)} + \frac{2|f|^2}{\nu^2 \lambda_1} \left\{ 1 - e^{-\nu \lambda_1 (t-s)} \right\}. \end{aligned}$$

Therefore, there exists  $T > s$  large enough such that for every  $u_0 \in B_0$  and  $\eta \in Q_\lambda B_0$  the solution  $u_2$  to the second equation in (3.1) satisfies

$$\|u_2(t)\|^2 \leq \frac{3|f|^2}{\nu^2 \lambda_1} \quad \text{for} \quad t > T.$$

Thus, equations (3.1) are dissipative. □

Note that (3.23) shows in the case of continuous data assimilation that  $|u_1(t) - u_2(t)| \rightarrow 0$  as  $t \rightarrow \infty$  implies  $|f_1(t) - f_2(t)| \rightarrow 0$  as  $t \rightarrow \infty$ . This same implication does not hold for two solutions  $u_1$  and  $u_2$  of the Navier–Stokes equations with respective time-dependent forcing functions  $f_1$  and  $f_2$  in general. Consider the following simple example. Let

$$u_1 = \left( \begin{array}{c} 0 \\ (t+1)^{-1} \sin(t+1)^2 \end{array} \right) \cos(x)$$

and

$$u_2 = \begin{pmatrix} (t+1)^{-1} \cos(t+1)^2 \\ 0 \end{pmatrix} \cos(y).$$

Then  $u_1$  and  $u_2$  are solutions of (2.6) with

$$f_1 = \begin{pmatrix} 0 \\ 2 \cos(t+1)^2 - (t+1)^{-2} \sin(t+1)^2 + \nu(t+1)^{-1} \sin(t+1)^2 \end{pmatrix} \cos(x)$$

and

$$f_2 = \begin{pmatrix} -2 \sin(t+1)^2 - (t+1)^{-2} \cos(t+1)^2 + \nu(t+1)^{-1} \cos(t+1)^2 \\ 0 \end{pmatrix} \cos(y).$$

Clearly  $\|u_1(t) - u_2(t)\|_\alpha \rightarrow 0$  as  $t \rightarrow \infty$  for any  $\alpha$ , however

$$|f_1 - f_2|^2 = |f_1|^2 + |f_2|^2 \sim 4 \quad \text{as } t \rightarrow \infty.$$

Therefore,  $|f_1(t) - f_2(t)|$  need not converge to zero as  $t \rightarrow \infty$  even though  $\|u_1(t) - u_2(t)\|_\alpha \rightarrow 0$  as  $t \rightarrow \infty$  for any  $\alpha$ . This implies that Theorem 1.4, Theorem 1.5 and Theorem 3.3 cover situations where the hypothesis of Theorem 1.3 are violated. Similar examples can be constructed using spatial oscillations whose length scales decrease over time. For these examples  $\|u_1 - u_2\| \rightarrow 0$  but  $|Q_\lambda f_1 - Q_\lambda f_2|$  does not converge to zero for any  $\lambda$ .

#### 4. Numerical Results

In this section we study numerically how the length scales present in the forcing function  $f$  affect the rate of continuous data assimilation and the number of determining modes. It is worth mentioning that almost all the previous analytical studies concerning the number of degrees of freedom in turbulent flow have focused on the Grashof number and almost none have addressed the effect of the spatial structure of the forcing on the dynamics. However, there were some computational results that took the structure of the forcing into consideration. See, for example, the work of Marchioro [37], Jolly [29], Platt, Sirovich and Fitzmaurice [38] and references therein.

Let  $\mathcal{G}(R)$  and  $\mathcal{F}(\lambda_f)$  be as given in the introduction. Thus,  $\mathcal{G}(R)$  is the set of all time-independent forcing functions  $f$  with Grashof number  $\text{Gr}(f) = R$  and  $\mathcal{F}(\lambda_f)$  is the subset of  $\mathcal{G}(R)$  consisting of the time-independent forcing functions that are supported on an annulus in Fourier space centered at  $\lambda_f$  of the form (1.11). All computational experiments were performed with  $\nu = 0.0001$  and  $\eta = 0$  on the  $2\pi$ -periodic torus for forcing functions with a Grashof number of  $R = 250000$ . Our computational results consist of two sets of experiments.

For our first experiment we select functions from  $\mathcal{F}(\lambda_f)$  for values of  $\lambda_f$  ranging from 25 through 625. We work in the vorticity representation. Thus, any  $f \in \mathcal{F}(\lambda_f)$  may be specified in terms of  $g = \nabla \times f$  according to

$$\hat{f}_k = \frac{\hat{g}_k}{k_1^2 + k_2^2} \begin{bmatrix} -ik_2 \\ ik_1 \end{bmatrix} \quad \text{where} \quad g = \sum_{\lambda_m \leq k^2 \leq \lambda_M} \hat{g}_k \phi_k. \quad (4.1)$$

To obtain a representative function  $f \in \mathcal{F}(\lambda_f)$  for each value of  $\lambda_f$  under consideration, we take the Fourier coefficients  $g_k$  to be Gaussian distributed, subject to the reality condition  $\hat{g}_k = \overline{\hat{g}_{-k}}$  and normalized so that  $|f| = 0.0025$ .

The initial condition  $u_0$  for each continuous data assimilation experiment was chosen so that it faithfully reflects the long term energetics of the forcing. This was done by integrating the Navier–Stokes equations (2.6) starting at time  $t = -25000$  with  $u_1(-25000) = 0$  until time  $t = 0$ . Figure 1 shows the time evolution of  $\|u_1\|$ ,  $|u_1|$  and  $\|u_1\|_*$  for a forcing function with  $\lambda_f = 25$ . By the end of the run these quantities have reached their statistically stationary states. Thus, one can assume that  $u_0 = u_1(0)$  is on the attractor. We note that as long as  $u_0$  reflects the long term energetics of the forcing the exact method of its choice is not important.

Given a particular forcing function and initial condition  $u_0$  the data assimilation parameter  $\lambda$  for  $P_\lambda$  in (3.1) was then varied to determine its effect on the time evolution of  $\|u_1 - u_2\|$ . As suggested by the bounds in Theorem 3.3 and illustrated in Figure 2, convergence, when it occurs, is exponential in time. Although convergence is not always monotonic, it is, on average, exponential. Therefore, a least squares fit of  $A \exp(-\alpha t)$  to  $\|u_1 - u_2\|$  was made for each computation to obtain the rate of continuous data assimilation  $\alpha$ . Values of  $\alpha$  as a function of  $\lambda$  are given in Figure 3 for the experiments with  $\lambda_f \leq 361$  and in Figure 4 for the experiments with  $\lambda_f \geq 361$ .

To provide a definite numerical criterion for deducing the number of determining modes, let  $\lambda_c$  be the smallest value of  $\lambda$  for which the corresponding rate of continuous data assimilation  $\alpha$  satisfies  $\alpha \geq 0.0005$ . We take the number of determining modes  $N_c$  to be the rank of  $P_\lambda$  for  $\lambda = \lambda_c$ . Table 1 summarizes how the number of determining modes depends on the length scales present in the forcing. Notice that the number of determining modes increases as  $\lambda_f$  increases from 25 through 361 but then decreases as  $\lambda_f$  increases from 361 through 625. We remark that the distances between successive values of  $\lambda_f$  have been chosen to be spaced far enough apart to guarantee that  $\|f\|_*$  will decrease monotonically as  $\lambda_f$  increases.

To compare these results with our theory, substitute (1.12) into (1.10) and use the bounds on  $c_1$  given in Lemma 2.3 to obtain

$$\begin{aligned} \lambda_c &\leq \min \{c_1^2 \nu^{-4} \|f\|_*^2, c_1 \nu^{-2} |f|\} \\ &\leq c_1 \nu^{-2} |f| \min \{c_1 \nu^{-2} |f| (\lambda_f^{1/2} - 1)^{-2}, 1\} \\ &\leq 539789 \min \{539789 (\lambda_f^{1/2} - 1)^{-2}, 1\}. \end{aligned}$$

Hence, when  $\lambda_f \geq 541260$  the first term in the minimum dominates, and our analytical bound on  $\lambda_c$  and consequently on  $N_c$  decreases as  $\lambda_f$  increases. In particular, our analytical estimate on the number of determining modes reaches zero for  $\lambda_f$  large enough. Although our computational estimates are much smaller and start decreasing long before our theoretical bounds do, it seems reasonable that the observed decrease in number of determining modes when forcing on smaller and smaller scales is still explained by the smallness of the  $V'$  norm of  $f$  when  $\lambda_f$  is large.

Something unexplained by our analysis appears to be happening for values of  $\lambda_f$  between 25 and 361. The number of determining modes increases as  $\lambda_f$  increases. In



an intuitive sense, this can be seen as an extrapolation of the fact that when  $\lambda_f = 0.7$  Theorem 1.7 implies that the dynamics are trivial. To shed further light on this case let us first examine the energy spectra of the reference calculations. Let

$$E(r) = L^2 \sum_{k \in \mathcal{J}_r} |\hat{u}_k|^2$$

where  $\mathcal{J}_r = \{k \in \mathcal{J} : r - 1/2 < |k| \leq r + 1/2\}$  and define

$$\langle E(r) \rangle = \lim_{T \rightarrow \infty} \frac{1}{T} \int_0^T E(r) dt.$$

The average energy spectrum of the reference calculation  $u_1$  corresponding to each of the forcing functions in Table 1 is shown in Figure 5. Here we have estimated the limit at  $T \rightarrow \infty$  by taking  $T = 10000$ . Note that as  $\lambda_f$  increases, the amount of energy in the high modes increases and a peak around  $\lambda_f$  becomes apparent. Also note that the total energy in the low modes decreases as  $\lambda_f$  increases.

Thus, there are two plausible explanations for the observed increase in the number of determining modes as  $\lambda_f$  ranges from 25 to 361. This increase might be caused by an increase of energy in the high modes of  $u_1$  or it might be caused by a decrease of energy in the low modes. If we suppose that the small scales are generated from the large scales, then a decrease of energy in the low modes would leave less large scale motion to generate the small scales, and therefore lead to an increase in the number of determining modes. To test this hypothesis a second set of experiments was conducted.

Given  $f_L \in \mathcal{F}(25)$  and  $f_H \in \mathcal{F}(484)$  we set  $f = \theta_L f_L + \theta_H f_H$  where  $\theta_L^2 + \theta_H^2 = 1$ . In this way we obtain forcing functions that are supported on two disjoint annuli in Fourier space—one on small wave numbers, the other on large. Here  $\theta_L$  and  $\theta_H$  are parameters determining the relative weights of the large and small length scales in the forcing. When  $\theta_H$  is close to zero  $f$  may be viewed as the perturbation of the large scales  $f_L$  by the small scales  $f_H$ ; when  $\theta_L$  is close to zero  $f$  is the perturbation of the small scales  $f_H$  by the large scales  $f_L$ . The values of  $\alpha$  for these computations are presented graphically in Figure 6. Table 2 indicates how the number of determining modes depends on  $\theta_L$  and  $\theta_H$ . Note that the perturbation of the large scales  $f_L$  by the small scales  $f_H$  does not significantly change the number of determining modes, whereas the perturbation of the small scales  $f_H$  by the large scales  $f_L$  dramatically affects the number of determining modes. This is consistent with our hypothesis that it is the absence of the large scales in the forcing which are primarily responsible for the increase in number of determining modes as  $\lambda_f$  ranges from 25 through 361 in the first set of experiments.

Further evidence in support of this hypothesis may be obtained by examining the averaged energy spectrum in Figure 7 of the reference calculation  $u_1$  corresponding to each of the forcing functions in Table 2. The most dramatic changes in the number of determining modes corresponds primarily to changes in the energy of the low modes of the energy spectrum.

It is amusing to note that the first three columns in Table 2 are qualitatively unchanged by taking  $\theta_H = 1$  in each of them. In this case we obtain a sequence of forcing

functions that increases in all norms while at the same time the corresponding number of determining modes decrease. A discussion of this seeming paradox and an explanation for it in terms of a Reynolds number based on the observational measurements  $P_\lambda u_1(t)$  shall be explored, if efficable, in a future work.

## 5. Computational Methods

Numerical computations for this paper were carried out using a C code written by the authors in conjunction with the Fourier transform library of Frigo and Johnson [26]. The actual calculations were made on microcomputers running the GNU/Linux operating system and LAM/MPI at the University of Nevada, Reno and at the University of California, Irvine. Correct behavior of our code was verified by comparison to existing programs written by Mike Jolly and Stephen Montgomery.

We use a spectral Galerkin method and compute the two-dimensional incompressible Navier–Stokes equations in its vorticity form

$$\frac{\partial \omega}{\partial t} - \nu \Delta \omega + (u \cdot \nabla) \omega = g \quad (5.1)$$

where  $\omega = \nabla \times u$  and  $g = \nabla \times f$ . Note that the one-third rule was used avoid aliasing, see Canuto, Hussaini, Quarteroni and Zang [3]. In terms of its Fourier decomposition (5.1) becomes

$$\frac{d\hat{\omega}_k}{dt} + \nu k^2 \hat{\omega}_k + ik \cdot \widehat{u\omega}_k = \hat{g}_k. \quad (5.2)$$

Following Henshaw, Kreiss and Reyna in [27], we integrate the dissipative term explicitly to obtain

$$\frac{d}{dt} \left\{ \hat{\omega}_k \exp(\nu k^2 t) \right\} + ik \cdot \widehat{u\omega}_k \exp(\nu k^2 t) = \hat{g}_k \exp(\nu k^2 t) \quad (5.3)$$

and then integrate the remaining terms using a third order Adams–Bashforth scheme. Initial time steps are computed via a fourth order Runge–Kutta scheme.

Let  $\hat{w}^j$  denote the Fourier transformed vorticity at time  $t_j = j\Delta t$ . Let

$$\Lambda = \text{diag}(\dots, \nu(k_1^2 + k_2^2), \dots)$$

and

$$F(t, \hat{w}) = -ik \cdot \widehat{u\omega}_k + \hat{g}_k.$$

Using these notations, the fourth order Runge–Kutta scheme used in our calculations may be written

$$\begin{aligned} K_1 &= F(t_j, \hat{w}^j) \\ K_2 &= F(t_j + \Delta t/2, e^{-\Lambda \Delta t/2}(\hat{w}^j + K_1 \Delta t/2)) \\ K_3 &= F(t_j + \Delta t/2, e^{-\Lambda \Delta t/2} \hat{w}^j + K_2 \Delta t/2) \\ K_4 &= F(t_j + \Delta t, e^{-\Lambda \Delta t} \hat{w}^j + e^{-\Lambda \Delta t/2} K_3 \Delta t) \\ \hat{w}^{j+1} &= e^{-\Lambda \Delta t} \hat{w}^j + (\Delta t/6)(e^{-\Lambda \Delta t} K_1 + 2e^{-\Lambda \Delta t/2}(K_2 + K_3) + K_4) \end{aligned}$$

and the third order Adams–Bashforth scheme may be written

$$\hat{w}^{j+1} = e^{-\Lambda\Delta t}\hat{w}^j + \frac{\Delta t}{12} \left\{ 23e^{-\Lambda\Delta t}F(t_j, \hat{w}^j) - 16e^{-2\Lambda\Delta t}F(t_{j-1}, \hat{w}^{j-1}) + 5e^{-3\Lambda\Delta t}F(t_{j-2}, \hat{w}^{j-2}) \right\}.$$

In our analysis, the forcing function  $f$  and the dynamical equations governing the evolution of  $u_1$  were assumed to be known exactly. Furthermore, the observable measurements  $P_\lambda u_1(t)$  were assumed to be error free. Therefore, if  $u_1(t)$  and  $u_2(t)$  happen to be equal at any time  $t$ , then they will remain equal for all subsequent times.

We would like our numerical computations to reflect these assumptions as closely as possible. To ensure our computations of  $u_1$  and  $u_2$  are identical, we discretize the equations governing  $u_1$  and  $u_2$  in exactly the same way and use the same executable program to compute each solution. This avoids any variations in automatic compile-time optimizations. Furthermore, we explicitly specify the processor dependent run-time optimizations used by the Fourier transform library [26]. Additional care was taken when implementing the continuous data assimilation to ensure that the exact values of  $P_\lambda u_1$  were used in a way that doesn't affect the discrete dynamics. Thus, since we are using a three step method for the time integrator, if the numerical solutions  $u_1(t)$  and  $u_2(t)$  are bit for bit equal at any three consecutive times  $t_j$ ,  $t_{j-1}$  and  $t_{j-2}$ , then they will remain bit for bit equal for all subsequent times.

To ensure sufficient computational resolution and stability, the CFL condition and the condition on the degrees of freedom in two-dimensional turbulence given in [27] were monitored for all computational runs. Let  $n$  by  $n$  be the grid size in physical space and  $\Delta t$  be the size of the time step. Let  $u$  and  $v$  be the  $x$  and  $y$  components of Eulerian velocity field. The CFL condition may be expressed as

$$\text{CFL} = \frac{n\Delta t}{2L} \sup_{x \in \Omega} \{|u| + |v|\} \leq 1$$

and the condition on degrees of freedom may be expressed as

$$k_{\max} = \nu^{-1/2} \sup_{x \in \Omega} \left\{ \left| \frac{\partial u}{\partial x} \right|, \left| \frac{\partial v}{\partial x} \right|, \left| \frac{\partial u}{\partial y} \right|, \left| \frac{\partial v}{\partial y} \right| \right\}^{1/2} \leq \frac{n\pi}{L}.$$

For our final calculations we took  $\nu = 0.0001$ ,  $L = 2\pi$ ,  $n = 169$  and  $\Delta t = 0.04$ . Thus, the Fourier transforms used to evaluate the non-linear term were performed on a 256 by 256 spatial grid. Given these parameters, our final calculations obeyed

$$\text{CFL} \leq 0.92 \quad \text{and} \quad k_{\max} \leq 82$$

and should, therefore, be well resolved.

Dependence of our numerical results on resolution was also studied directly. It should be noted that our experiment involves integrating a system with sensitive dependence on its initial conditions over a very long period of time. Thus, given different

values for  $n$  and  $\Delta t$  otherwise identical calculations of  $u_1$  will differ after long enough time. Even for identical values of  $n$  and  $\Delta t$  these calculations were observed to differ depending on the compiler and level of optimization used. The best we can hope for is that statistical properties including the rate of continuous data assimilation and number of determining modes remain unchanged. A number of preliminary tests with  $f$ ,  $\lambda$  and  $u_0$  fixed were made to determine how our results depend on the exact values of  $n$  and  $\Delta t$ . Figure 9 illustrates the evolution of  $\|u_1 - u_2\|$  for a set of resolution tests. These tests were conducted with the data assimilation parameter  $\lambda = 26$  and the forcing function from Table 1 with  $\lambda_f = 64$ . It is clear that the rate of continuous data assimilation is independent of the resolution of the computation. Thus, we hope that our results are reasonably free from numerical artifacts.

Recall that the amplitudes of the Fourier components of  $f$  were chosen randomly with respect to a Gaussian distribution. Thus, our exact choice of  $f$  for each experiment was somewhat arbitrary. Table 3 explores for  $\lambda_f = 64$  how the randomness in our choice of Fourier components for  $f$  affect the rate of continuous data assimilation. Notice that the  $V$  and  $V'$  norms of  $f$  vary by about one percent while the resulting rate of continuous data assimilation  $\alpha$  varies by about three percent. We suppose all our results are within this margin for any reasonably probable choice of  $f$ .

**Table 3.** Different versions of forcing functions supported on the length scales around  $\lambda_f = 64$ . The rate  $\alpha$  was measured for continuous data assimilation on  $N = 88$  modes.

Version	$\ f\ $	$ f $	$\ f\ _*$	$\alpha$
1	0.01928	0.0025	0.0003272	0.0105127
2	0.01905	0.0025	0.0003309	0.0102093
3	0.01921	0.0025	0.0003287	0.0099258
4	0.01923	0.0025	0.0003282	0.0104484
5	0.01919	0.0025	0.0003292	0.0112591

An essential feature of a typical forcing function is that the spatial length scales are clearly exhibited while at the same time there are no additional symmetries. This feature is illustrated in Figure 8 which gives the constant level curves of  $\nabla \times f$  for the forcing function with  $\lambda_f = 64$  from Table 1. If, for example,  $f$  had additional periodic structure, then the initial condition  $u_0$  and consequently  $u_1$  and  $u_2$  would also have this periodic structure. Thus, a rescaling such as in (1.8) would be possible. One could not expect the results from Table 1 to be relevant for such forcing functions.

One final remark is on our procedure for determining  $\lambda_c$  experimentally. Recall that  $\lambda_c$  was defined to be the smallest value of  $\lambda$  such that  $\alpha \geq 0.0005$ . This cutoff was chosen simply so that the evolution of  $\|u_1 - u_2\|$  need not be computed for times much greater than  $t = 25000$  to distinguish cases of convergence from non-convergence. Therefore, it is possible that smaller values of  $\lambda$  would also show convergence. In such cases our  $\lambda_c$  still provides an upper bound on the number of determining modes, only perhaps not quite as sharp as possible.

## 6. Acknowledgments

This work was supported in part by the National Science Foundation under grants number DMS-9902360, DMS-9706964, DMS-9704632 and DMS-0204794. Partial support was also provided by the US Civilian Research and Development Foundation (CRDF) Cooperative Grants Program under grant number RM1-2343-MO-02. This work was completed while E.S.T. was the Stanislaw M. Ulam Visiting Scholar at the Center for Nonlinear Studies in the Los Alamos National Laboratory.

## 7. References

- [1] J.P. Aubin, Un théorème de compacité, *C.R. Acad. Sci. Paris Sér. I Math.*, **256** (1963), 5042–5044.
- [2] G.L. Browning, W.D. Henshaw, H.O. Kreiss, A Numerical Investigation of the Interaction between the Large and Small Scales of the Two-Dimensional Incompressible Navier–Stokes Equations, UCLA CAM Technical Report 98–23, [ftp://ftp.math.ucla.edu/pub/camreport/cam98-23\[a-d\].ps.gz](ftp://ftp.math.ucla.edu/pub/camreport/cam98-23[a-d].ps.gz), April 1998.
- [3] C. Canuto, M.Y. Hussaini, A. Quarteroni, T.A. Zang, *Spectral Methods in Fluid Dynamics*, Springer Series in Computational Physics, Springer-Verlag, 1988.
- [4] C. Cao, M.A. Rammaha, E.S. Titi, The Navier-Stokes equations on the rotating 2D sphere: Gevrey regularity and asymptotic degrees of freedom, *Zeitschrift für Angewandte Mathematik and Physik*, **50** (1999) 341–360.
- [5] J. Charney, M. Halem, R. Jastrow, Use of incomplete historical data to infer the present state of the atmosphere, *J. Atmos. Sci.*, **26** (1969) 1160–1163.
- [6] B. Cockburn, D.A. Jones, E.S. Titi, Determining degrees of freedom for nonlinear dissipative equations, *C. R. Acad. Sci. Paris Sér. I Math.*, **321** (1995), no. 5, 563–568.
- [7] B. Cockburn, D.A. Jones, E.S. Titi, Estimating the number of asymptotic degrees of freedom for nonlinear dissipative systems, *Math. Comp.*, **66** (1997), no. 219, 1073–1087.
- [8] P. Constantin, C.R. Doering, E.S. Titi, Rigorous estimates of small scales in turbulent flows, *J. Math. Phys.*, **37** (1996), no. 12, 6152–6156.
- [9] P. Constantin, C. Foias, *Navier–Stokes equations*, Chicago Lectures in Mathematics. University of Chicago Press, Chicago, IL, 1988.
- [10] P. Constantin, C. Foias, O.P. Manley, Effects of the forcing function spectrum on the energy spectrum in 2-D turbulence, *Phys. Fluids*, **6** (1994), no. 1, 427–429.
- [11] P. Constantin, C. Foias, R. Temam, On the dimension of the attractors in two-dimensional turbulence, *Phys. D*, **30** (1988), no. 3, 284–296.
- [12] R. Daley, *Atmospheric Data Analysis*, Cambridge Atmospheric and Space Science Series, Cambridge University Press, 1991.
- [13] A. Debussche, M. Marion, On the construction of families of approximate inertial manifolds, *J. Differential Equations*, **100** (1992), 173–201.

- [14] C. Devulder, M. Marion, A class of numerical algorithms for large time integration: the nonlinear Galerkin methods, *SIAM J. Numer. Anal.*, **29** (1992), 462–483.
- [15] C. Devulder, M. Marion, E.S. Titi, On the rate of convergence on the nonlinear Galerkin methods, *Mathematics of Computation*, **60** (1993), no. 202, 495–514.
- [16] C.R. Doering, J.D. Gibbon, *Applied Analysis of the Navier–Stokes Equations*, Cambridge Texts in Applied Mathematics, Cambridge University Press, 1995.
- [17] T. Debios, F. Jauberteau, R. Temam, The nonlinear Galerkin method for the two and three-dimensional Navier–Stokes equations. *Twelfth International Conference on Numerical Methods in Fluid Dynamics (Oxford, 1990)*, 116–120, Lecture Notes in Phys. 371, Springer, 1990.
- [18] C. Foias, M.S. Jolly, I.G. Kevrekidis, G.R. Sell, E.S. Titi, On the computation of inertial manifolds, *Phys. Lett. A*, **31** (1988), 433–436.
- [19] C. Foias, O.P. Manley, R. Temam, Approximate inertial manifolds and effective viscosity in turbulent flows. *Phys. Fluids A*, **3** (1991), no. 5, part 1, 898–911.
- [20] C. Foias, O.P. Manley, R. Temam, Iterated approximate inertial manifolds for Navier–Stokes equations in 2-D, *J. Math. Anal. Appl.*, **178:2** (1993), 567–583.
- [21] C. Foias, O.P. Manley, R. Temam, Y. Trève, Asymptotic analysis of the Navier–Stokes equations, *Phys. D*, **9** (1983), 157–188.
- [22] C. Foias, G. Prodi, Sur le comportement global des solutions non stationnaires des équations de Navier–Stokes en dimension two, *Rend. Sem. Mat. Univ. Padova*, **39** (1967), 1–34.
- [23] C. Foias, G.R. Sell, E.S. Titi, Exponential tracking and approximation of inertial manifolds for dissipative nonlinear equations, *J. Dynamics Differential Equations*, **1** (1989), 199–244.
- [24] C. Foias, R. Temam, Determination of the solutions of the Navier-Stokes equations by a set of nodal values, *Math. Comput.*, **43** (1984), 117–133.
- [25] C. Foias, R. Temam, The connection between the Navier-Stokes equations, dynamical systems, and turbulence theory. *Directions in partial differential equations (Madison, WI, 1985)*, 55–73, Publ. Math. Res. Center Univ. Wisconsin, 54, *Academic Press*, Boston, MA, 1987.
- [26] M. Frigo, S.G. Johnson, *The Fastest Fourier Transform in the West*, MIT Technical Report, MIT-LCS-TR-728, <http://www.fftw.org/>, 1997.
- [27] W.D. Henshaw, H.O. Kreiss, L.G. Reyna, On the Smallest Scale for the Incompressible Navier–Stokes Equations, *Theoretical and Computational Fluid Dynamics*, (1989) 1, 65–95.
- [28] M.J. Holst, E.S. Titi, Determining projections and functionals for weak solutions of the Navier-Stokes equations *Recent developments in optimization theory and nonlinear analysis*, (Jerusalem, 1995), 125–138, *Contemp. Math.*, 204, Amer. Math. Soc., Providence, RI, 1997.
- [29] M.S. Jolly, Bifurcation computations on an approximate inertial manifold for the 2D Navier–Stokes equations, *Phys. D*, **63** (1993), no. 1–2, 8–20.

- [30] M.S. Jolly, I.G. Kevrekidis, E.S. Titi, Approximate inertial manifolds for the Kuramoto–Sivashinsky equation: analysis and computations, *Phys. D*, **44** (1990), 38–60.
- [31] D.A. Jones, E.S. Titi, On the Number of Determining Nodes for the 2D Navier–Stokes Equations, *Journal of Mathematical Analysis and Applications*, **168** (1992), no. 1, 72–88.
- [32] D.A. Jones, E.S. Titi, Upper bounds on the number of determining modes, nodes, and volume elements for the Navier–Stokes equations, *Indiana Univ. Math. J.*, **42** (1993), no. 3, 875–887.
- [33] H.O. Kreiss, J. Yström, Numerical experiments on the interaction between large and small-scale motion of incompressible turbulent flows, *J. Fluid Mech.*, to appear.
- [34] O.A. Ladyzhenskaya, *The Mathematical Theory of Viscous Incompressible Flow*, Second English Edition, Translated from the Russian by Richard A. Silverman and John Chu, Mathematics and its Applications, Vol. 2, Gordon and Breach, Science Publishers, New York, 1969.
- [35] O.A. Ladyzhenskaya, On the dynamical system generated by the Navier–Stokes equations, *J. Soviet Math.*, **3** (1975), 458–479.
- [36] J.L. Lions, E. Magenes, *Nonhomogeneous Boundary Value Problems and Applications*, Springer, Berlin, 1972.
- [37] C. Marchioro, An example of absence of turbulence for any Reynolds number, *Comm. Math. Phys.*, **105** (1986), no. 1, 99–106.
- [38] N. Platt, L. Sirovich, N. Fitzmaurice, An investigation of chaotic Kolmogorov flows, *Phys. Fluids. A*, **3** (1991), 681–696.
- [39] J. Robinson, *Infinite-Dimensional Dynamical Systems: From Basic Concepts to Actual Calculations*, Cambridge Texts in Applied Mathematics, 2001.
- [40] R. Temam, *Navier–Stokes Equations: Theory and Numerical Analysis*, revised edition, AMS Chelsea Publishing, 1984.
- [41] R. Temam, *Navier–Stokes Equations and Nonlinear Functional Analysis*, second edition, CBMS-NSF Regional Conference Series in Applied Mathematics vol 66, SIAM, 1995.
- [42] E.S. Titi, On a criterion for locating stable stationary solutions to the Navier–Stokes equations, *Nonlinear Anal.*, **11** (1987), 1085–1102.
- [43] Y.M. Trève, O.P. Manley, Minimum number of modes in approximate solutions of equations of hydrodynamics, *Phys. Lett. A*, **82**, 88, 1981.

**Figure 1.** Evolution of  $\|u_1\|$ ,  $|u_1|$  and  $\|u_1\|_*$  for  $\lambda_f = 25$  shows that initial data for the continuous data assimilation experiment is very close to the global attractor.

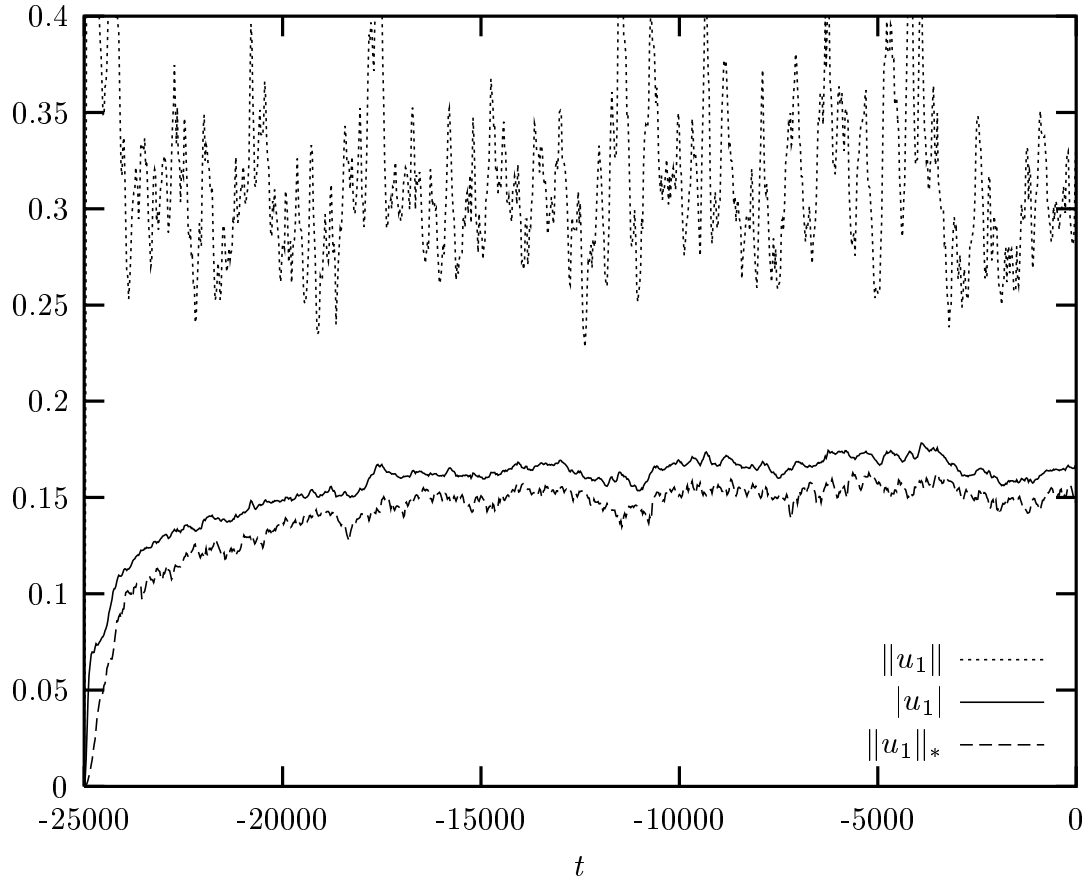




**Figure 2.** Evolution of  $\|u_1 - u_2\|$  with  $\lambda_f = 64$  for continuous data assimilation on  $N$  Fourier modes. Convergence, when it occurs, is exponential in time.

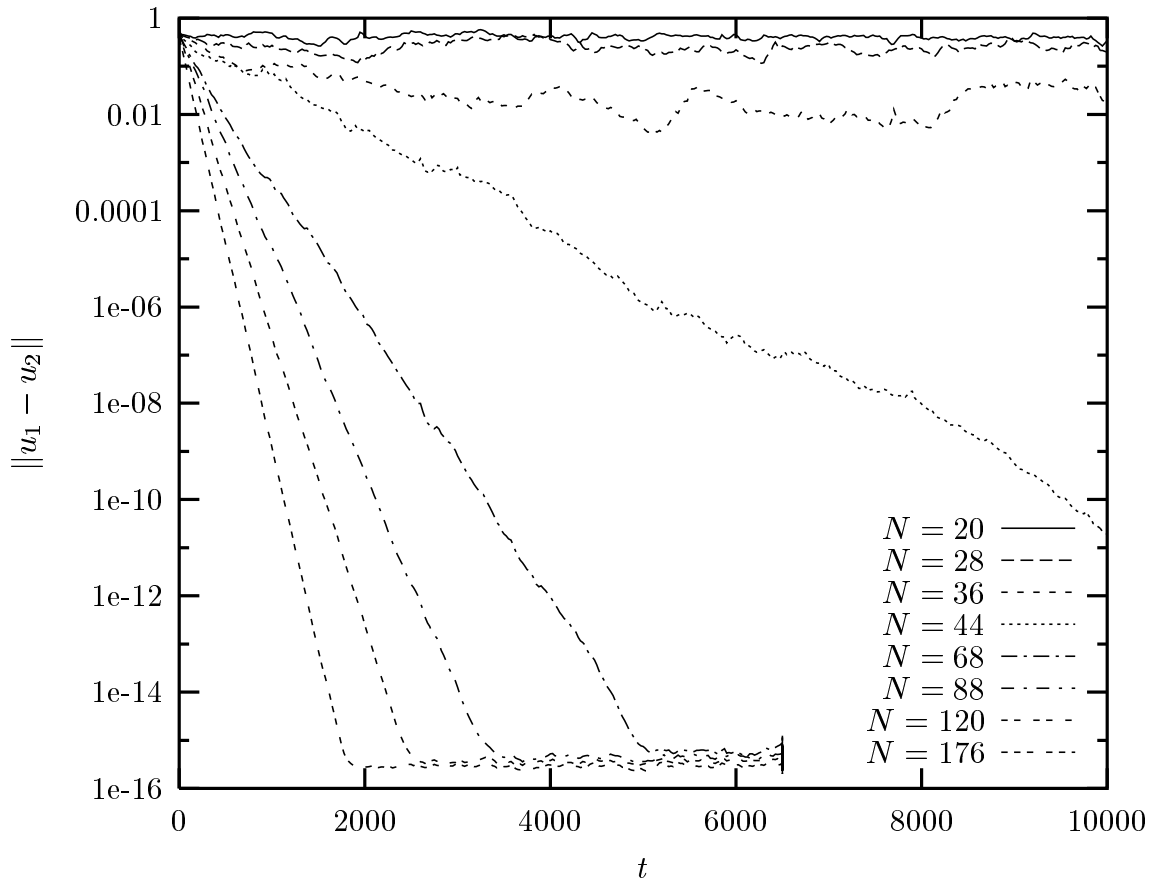


**Figure 3.** Rate of continuous data assimilation for forcing supported on length scales between  $\lambda_f = 25$  and 361. The horizontal line at  $\alpha = 0.0005$  represents the cutoff for deducing the number of determining modes.

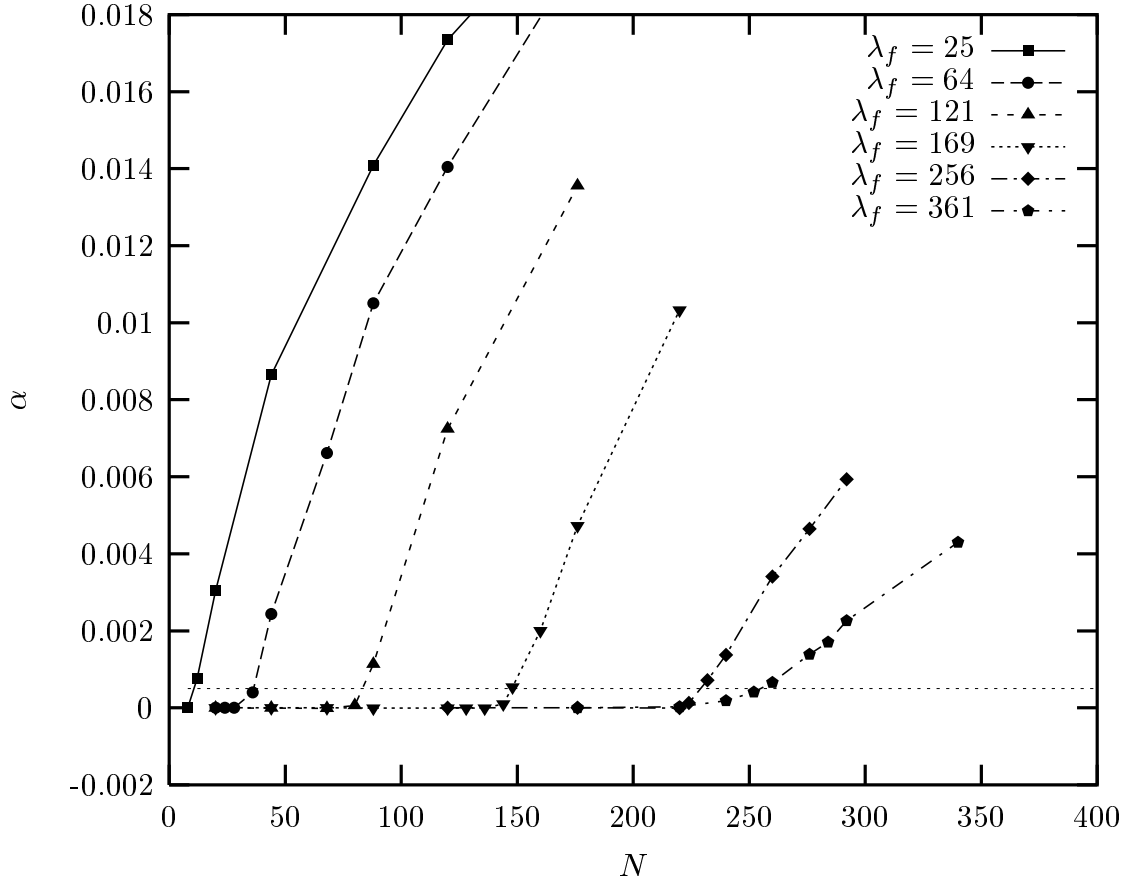


**Figure 4.** Rate of continuous data assimilation for forcing supported on length scales between  $\lambda_f = 361$  and 625. The horizontal line at  $\alpha = 0.0005$  represents the cutoff for deducing the number of determining modes.

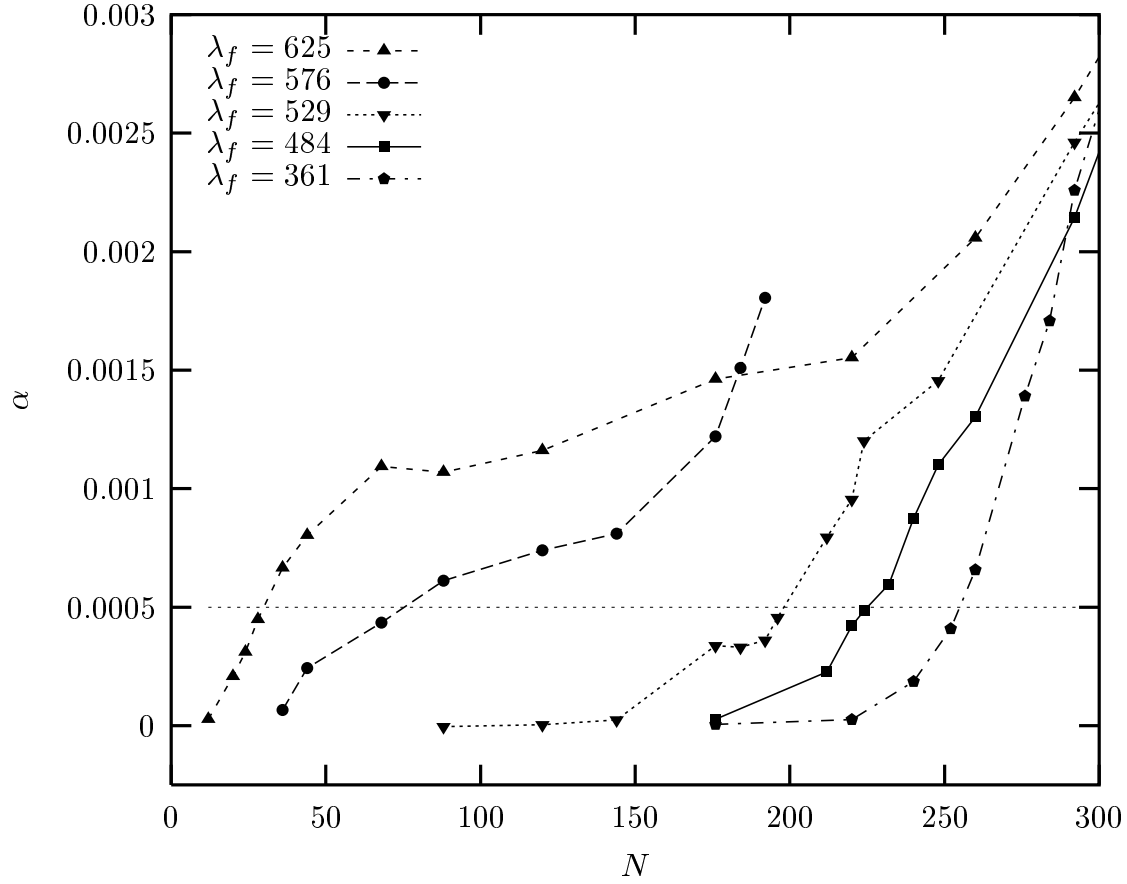


**Figure 5.** Time averages of the energy spectrum of  $u_1$  show a characteristic peak around  $\lambda_f$  for forcing functions supported on small length scales. The average was computed by taking  $T = 10000$ .

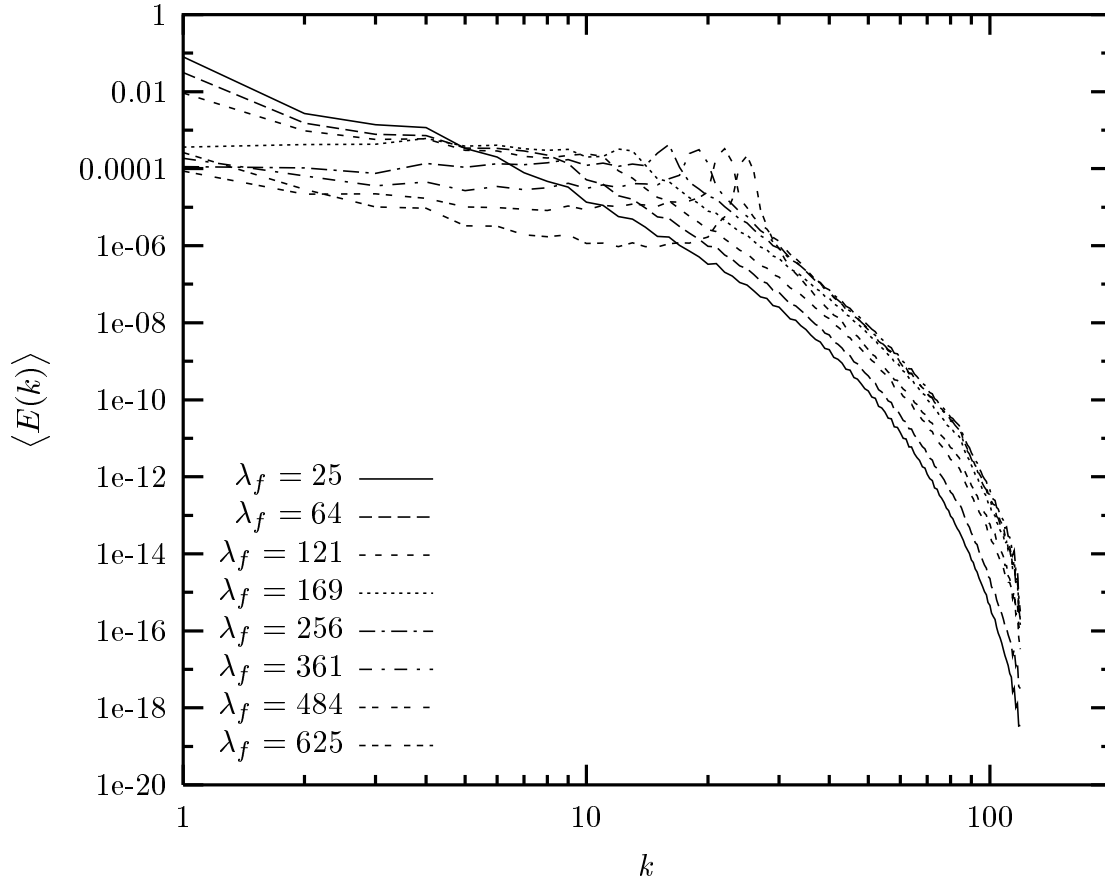


**Figure 6.** Rate of continuous data assimilation for the forcing function  $f = \theta_L f_L + \theta_H f_H$  where  $f_L \in \mathcal{F}(25)$  and  $f_H \in \mathcal{F}(484)$ . The horizontal line at  $\alpha = 0.0005$  represents the cutoff for deducing the number of determining modes.

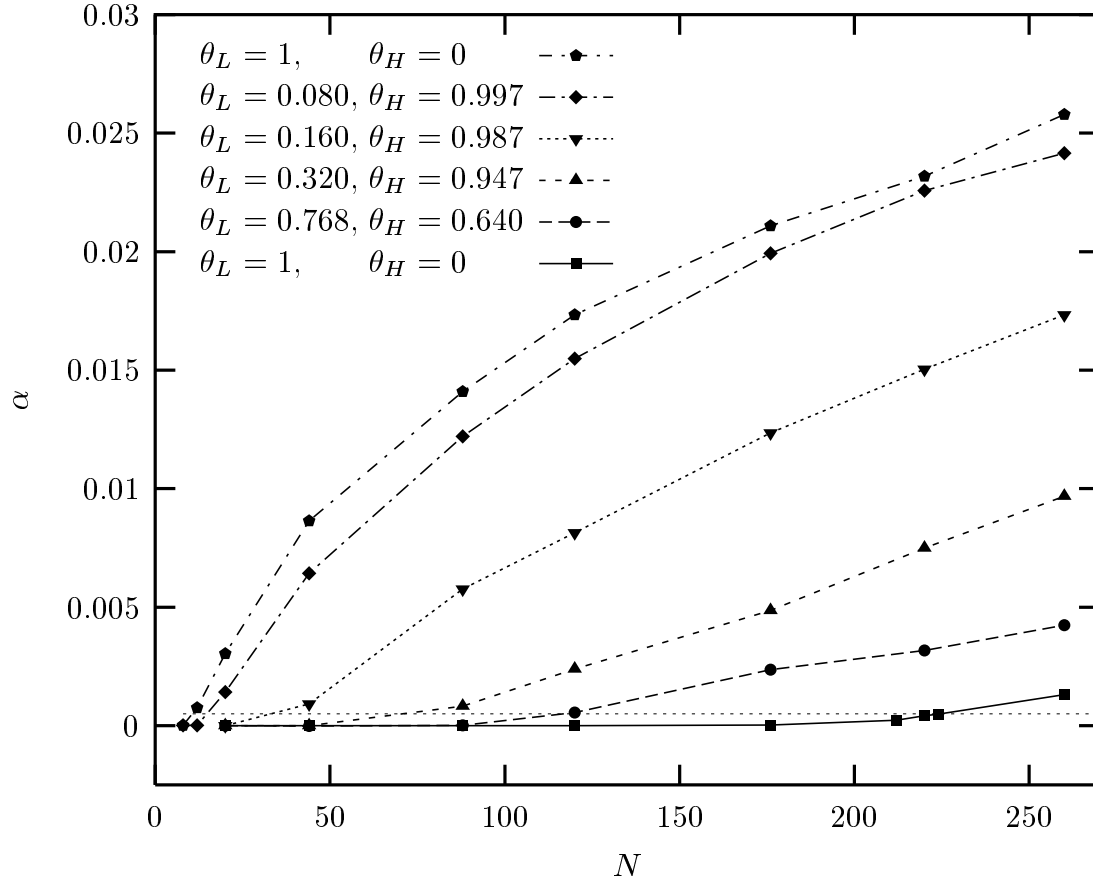


**Figure 7.** Time averages of the energy spectrum of  $u_1$  for  $f = \theta_L f_L + \theta_H f_H$  where  $f_L \in \mathcal{F}(25)$  and  $f_H \in \mathcal{F}(484)$ . The average was computed by taking  $T = 10000$ .

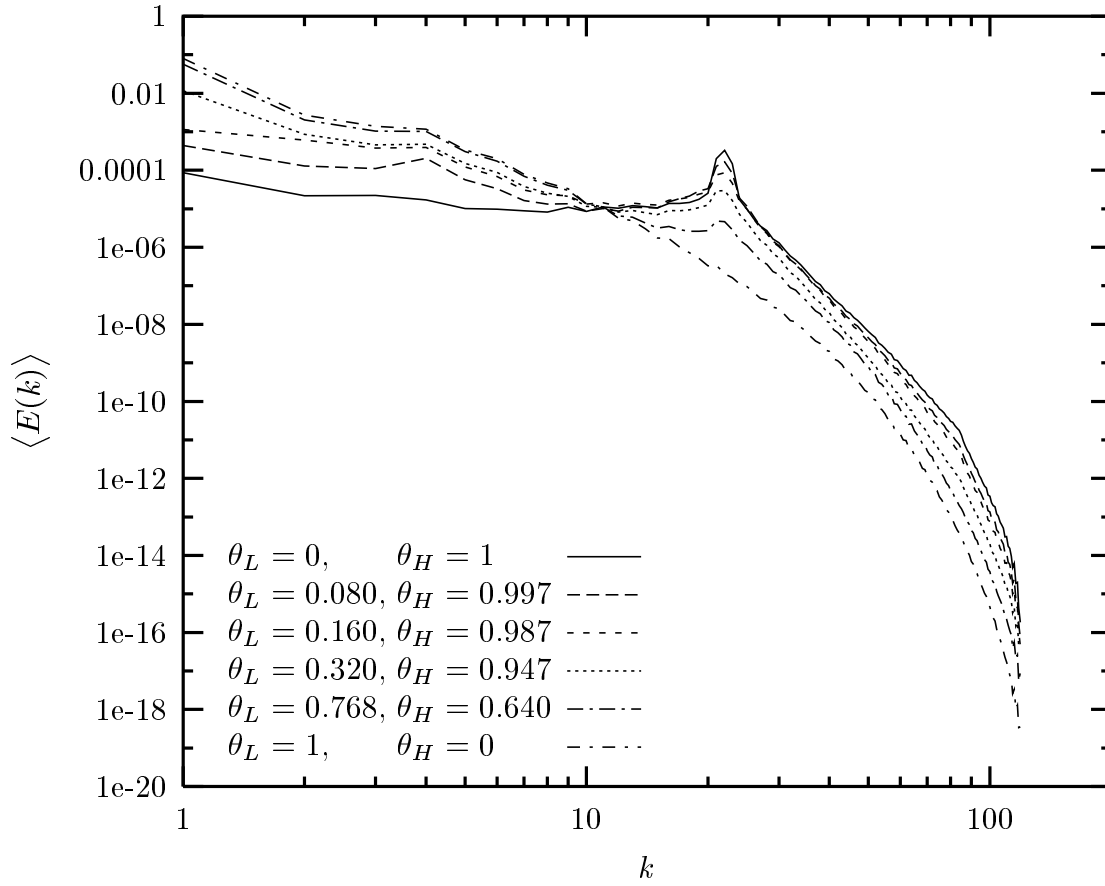


**Figure 8.** Constant level curves of  $g = \nabla \times f$  for  $\lambda_f = 64$  illustrate the length scales present in the forcing.

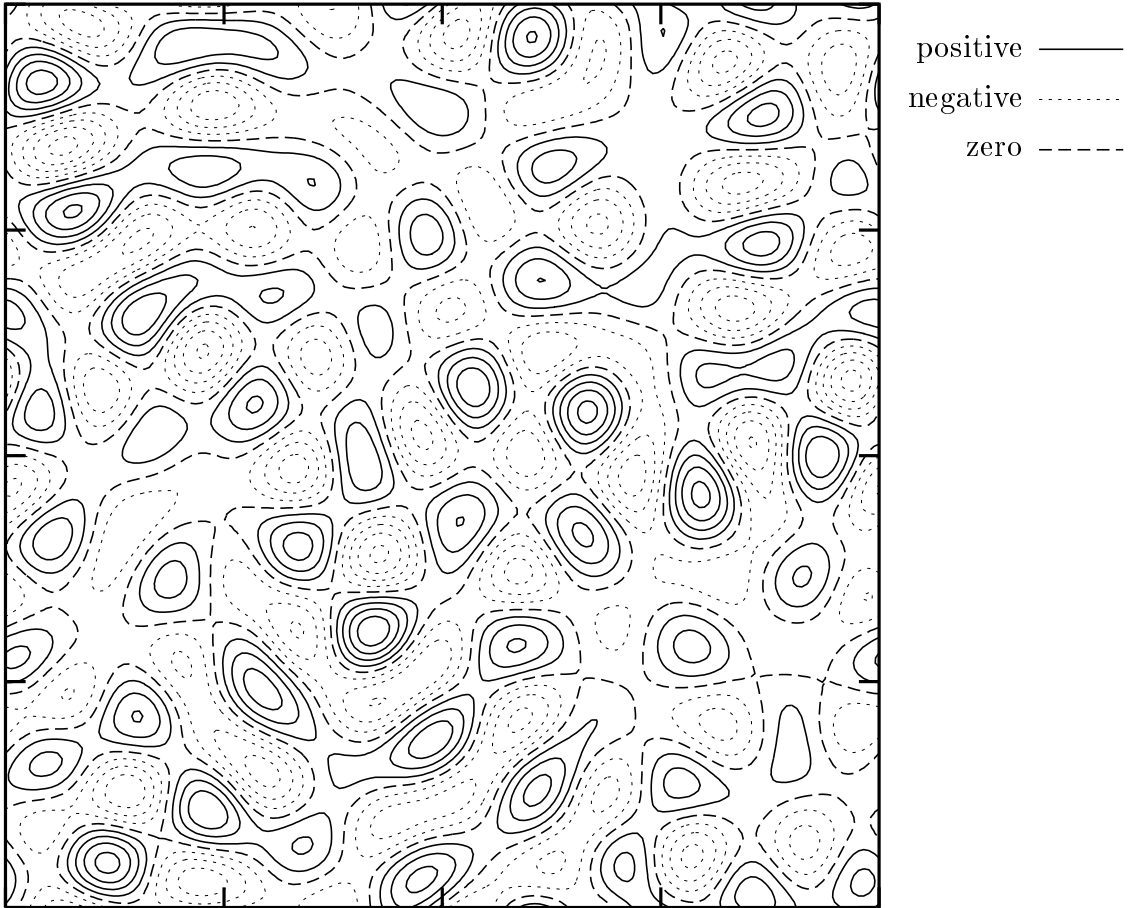


**Figure 9.** The evolution of  $\|u_1 - u_2\|$  for different values of  $n$  and  $\Delta t$  with  $\lambda = 26$  and  $\lambda_f = 64$  shows that the rate of continuous data assimilation is unrelated to the numerical resolution. The solid line represents the resolution of our final calculations. Other resolutions have been offset by decades for clarity.

